Integrated Master in Chemical Engineering

Hysteresis in Tyre Textile Reinforcements

Master's Thesis

by

Mariana Gomes

Developed within the course of dissertation

held in

Continental AG

Body Compound & Reinforcement Technology Department



Supervisor at FEUP: **Prof. Fernão Magalhães**

Supervisor at Continental: **Dr. Thomas Kramer**



Departamento de Engenharia Química

July of 2018

Confidential document. Use only for evaluation purposes

This master's thesis contains confidential information from Continental Reifen Deutschland GmbH. Duplication or distribution of the work, as well as the utilization or communication of its contents, is strictly prohibited without the express written authorization of Continental Reifen Deutschland GmbH, Jädekamp 30, 30419 Hanover.

Acknowledgement

To all who helped me bring this project to life, my most sincere gratitude:

To Dr. Thomas Kramer, for his availability, constant support and invaluable advice; and for the chance to explore such an inspiring topic, allowing me to discover the potential of R&D.

To Prof. Fernão Magalhães, for his helpful feedback and his guidance.

To everyone in the R&D Department, but especially Dr. Nermeen Nabih and Tiago Moura, for always making me feel welcome, as well as for all the friendly advice and support.

To Anuwat Suwannachit, Christian Neufeld and Andreas Maibohm, for including me in the team and for always being available to help.

To my family and my boyfriend, for keeping me company from miles away, for always being there when I needed a word of support or a smile, but especially for always believing in me.

- -

This work was funded by Continental Reifen Deutschland GmbH and by project POCI-01-0145-FEDER-006939 (Laboratory for Process Engineering, Environment, Biotechnology and Energy - UID/EQU/00511/2013) funded by the European Regional Development Fund (ERDF), through COMPETE2020 - Programa Operacional Competitividade e Internacionalização (POCI) and by national funds, through FCT - Fundação para a Ciência e a Tecnologia.



Abstract

The pneumatic tyre is a dominant solution in the automotive sector. It has remained so by being continuously innovated and optimised and, as such, several research efforts are made in the areas that allow and require further improvements.

As the main contributor to rolling resistance, hysteresis has been attracting the attention of developers and suppliers, being the focus of several recent studies, particularly with rubber, in order to reduce energy losses and therefore fuel consumption.

As such, the objective of this project was to develop a test method that would allow the determination and evaluation of the characteristic variables that describe hysteresis. For this purpose, the Dynamical Mechanical Analysis technique was applied in order to characterize this phenomenon in textile reinforcements, providing valuable information for further tyre optimisation.

Hysteresis properties of Nylon 6.6 cord reinforcements were evaluated as functions of temperature, frequency, linear density and twist. PET cords were used to evaluate the influence of the dip pick up percentage (DPU %).

Twist showed a negatively linear effect on the storage and loss moduli, presenting a negligible change for the overall damping capacity.
For linear density, all three characteristic variables indicated curvature, requiring further studies to determine the specific effect.
DPU % showed a very small impact on the hysteresis of the cords, only presenting a statistically significant effect for the storage modulus, following a negative linear correlation. Besides that, microscopical analysis of the cords' cross-sections showed no evidence of a difference in the dip penetration.
Additionally, a test procedure was developed and optimised in order to investigate the application of the Time-Temperature Superposition principle to textile cords.

Overall, this project allowed for a better understanding of the behaviour of textile reinforcements under dynamic conditions, as well as the study of influencing factors.

Keywords: textile cord, hysteresis, viscoelasticity.

Resumo

O pneu é uma solução dominante no setor automóvel. Tem-se assim mantido devido à sua contínua inovação e otimização e, como tal, vários esforços de pesquisa são realizados nas áreas que permitem e requerem melhorias.

Sendo o principal contribuinte para a resistência ao rolamento, a histerese tem atraído a atenção de responsáveis pelo desenvolvimento e fornecimento, sendo o foco de vários estudos recentes, especialmente relativos à borracha, a fim de reduzir perdas de energia e, consequentemente, o consumo de combustível.

Assim, o objetivo deste projeto foi desenvolver um método de teste que permitisse a determinação e avaliação das variáveis características que descrevem a histerese.
Para tal, utilizou-se a técnica de Análise Dinâmico-Mecânica, de modo a caracterizar este fenómeno no que diz respeito aos reforços têxteis, fornecendo informações relevantes para a otimização contínua dos pneus.

As propriedades histeréticas dos reforços de Nylon 6.6 foram avaliadas em função da temperatura, frequência, densidade linear e torção. Cordas de poliéster foram utilizadas para avaliar a influência da percentagem de impregnação (DPU %).

A torção apresentou um efeito linear negativo nos módulos de armazenamento e de perda, implicando, no entanto, uma mudança insignificante para a capacidade geral de amortecimento.
Quanto à densidade linear, as três variáveis características apresentam curvatura em função desta, exigindo estudos adicionais para determinar o efeito específico.
A DPU % apresentou um impacto muito pequeno na histerese das cordas, apresentando apenas um efeito estatisticamente significativo para o módulo de armazenamento, segundo uma correlação linear negativa. Além disso, a análise microscópica de secções transversais das cordas não mostrou nenhuma evidência de diferença na penetração da solução de impregnação.
Adicionalmente, um método de teste foi desenvolvido e otimizado para investigar a aplicação do princípio da Sobreposição Tempo-Temperatura aos reforços têxteis.

Em geral, este projeto permitiu uma melhor compreensão do comportamento de reforços têxteis em condições dinâmicas, assim como o estudo de fatores de influência.

Palavras-chave: corda têxtil, histerese, viscoelasticidade.

Declaration

I hereby declare, on my word of honour, that this work is original and that all non-original contributions were properly referenced with source identification.

Mariana Gonçalves de Seixas Gomes

July of 2018

Contents

1 Introduction **1**
1.1 Continental AG . . . 1
1.2 Motivation and contributions of the work . . . 1
1.3 Organization of the thesis . . . 2

2 Context and state of the art **3**
2.1 Overview of the modern tyre . . . 3
2.2 Materials used in a tyre . . . 3
2.3 Tyre components . . . 4
2.4 Textile reinforcements . . . 5
2.4.1 Rayon . . . 6
2.4.2 Nylon . . . 6
2.4.3 Polyester . . . 6
2.4.4 Aramid . . . 6
2.4.5 Hybrid . . . 7
2.5 Cord design . . . 7
2.6 Rolling resistance . . . 8
2.7 Hysteresis . . . 10
2.7.1 Elasticity and viscoelasticity . . . 10
2.7.2 Dynamic Mechanical Analysis . . . 12

3 Technical description **15**
3.1 Test system and basic procedure . . . 15
3.2 Testing and data analysis . . . 16
3.2.1 Setup optimisation . . . 17
3.2.2 Linear density and twist study . . . 18
3.2.3 Master curve construction . . . 20
3.2.4 DPU % study . . . 23

4 Results and discussion **24**
4.1 Setup optimisation . . . 24
4.2 Linear density and twist study . . . 28
4.3 Master curve construction . . . 33
4.4 DPU % study . . . 40

5 Conclusion **44**

6 Assessment of the work done **45**
6.1 Objectives achieved 45
6.2 Limitations and future work 45
6.3 Final assessment 46

References **47**

Appendix A Linear density and twist study **I**

Appendix B Master curve construction **III**

Appendix C DPU % study **IX**

List of Figures

1 Breakdown of ingredients from a summer tyre . . . 3
2 Tyre structure . . . 4
3 Elastic, viscoelastic, and viscous response to a load applied at time t_a and released at t_r . . . 11
4 Stress-strain plot for elastic and viscoelastic behaviour . . . 12
5 Stress and strain over time for a purely elastic material . . . 12
6 Stress and strain over time for a viscoelastic material . . . 13
7 Vectorial representation of the complex modulus . . . 14
8 MTS Acumen 3 Test System . . . 15
9 Tested clamping setups . . . 17
10 Example of the non linear regression of the data . . . 19
11 Construction of a master curve, from isothermal frequency sweeps . . . 20
12 Illustration of the test procedure by frequency and temperature steps . . . 21
13 Illustration of the nested frequency sweeps in a temperature sweep procedure, with decreasing temperature steps . . . 22
14 Force-elongation curves for Nylon 6.6 with a 940×2 construction, at 23 °C 24
15 Force-elongation curves for Nylon 6.6 with a 940×2 construction, at 100 °C 25
16 Force-elongation curves for Nylon 6.6 with a 940×2 construction, using the torque screwdriver or the pneumatic clamp setup . . . 26
17 Force-elongation curves for Nylon 6.6 with a 940×2 construction, with respect to different inlays . . . 27
18 Force-elongation curves for Nylon 6.6 with a 940×2 construction, using the pneumatic clamps with an aluminium inlay, with respect to different temperatures . . . 27
19 Force-elongation curves for Nylon 6.6 cords with variable twist and linear density . . . 28
20 Stress-strain curves for Nylon 6.6 cords with variable twist and linear density 29
21 Scatterplot of E' over twist . . . 30
22 Scatterplot of E'' over twist . . . 30
23 Scatterplot of $\tan\delta$ over twist . . . 31
24 Scatterplot of E' over linear density . . . 31
25 Scatterplot of E'' over linear density . . . 32
26 Scatterplot of $\tan\delta$ over linear density . . . 32
27 Representation of E' for the frequency and temperature steps test procedure 34

28 Representation of E' for temperature steps test procedure, as a frequency of 10 Hz is maintained throughout the entire test 36
29 Comparative results for E' from the nested frequency sweeps in a temperature sweep procedures 37
30 Plot of E', E'' and $\tan\delta$ over frequency at different temperatures 38
31 Plot of E', E'' and $\tan\delta$ over temperature at different frequencies 39
32 Scatterplot of E' over DPU % 40
33 Scatterplot of E'' over DPU % 41
34 Scatterplot of $\tan\delta$ over DPU % 41
35 Graph of the Tukey comparison for E' over DPU % 42
36 Linear regression fit for E' over DPU % 42
37 Analysis of residuals for E' over DPU % 43
38 Microscopic analysis of a cross section of the PET cords 43
39 Representation of E'' for the frequency and temperature steps test procedure III
40 Representation of $\tan\delta$ for the frequency and temperature steps test procedure IV
41 Comparative results for E'' from the nested frequency sweeps in a temperature sweep procedures V
42 Comparative results for $\tan\delta$ from the nested frequency sweeps in a temperature sweep procedures V

List of Tables

3 Cord characteristics for the linear density and twist study 18
4 Cord characteristics for the DPU % study 23
5 Design of experiments for the linear density and twist study, as well as the corresponding limit value estimates I
6 Obtained fitted values from the selected frequency and temperature sweep VI
7 Design of experiments for the DPU % study, as well as the corresponding limit value estimates IX
8 ANOVA output for E' as function of DPU % X
9 ANOVA output for E'' as function of DPU % X
10 ANOVA output for $\tan\delta$ as function of DPU % XI
11 Regression output for E' as function of DPU % XII

Glossary

Sign	Description	Unit
ε	Stress	$\mathrm{N/mm^2}$
σ	Strain	%
F	Force	N
t	Time	h
l	Length	mm
T	Temperature	°C
ω	Frequency	Hz
A	Area	$\mathrm{mm^2}$
E'	Storage modulus	$\mathrm{N/mm^2}$
E''	Loss modulus	$\mathrm{N/mm^2}$
δ	Phase shift	°
$\tan\delta$	Loss factor	
τ	Torque	$N \cdot m$
	Twist	tpm
TF	Twist factor	
LD	Linear density	dtex
M_{dc}	Mass of the dipped cord	g
M_{d}	Mass of the dip	g
DPU	Dip pick up	%
a_T	Shift factor	
α	Significance level	

Acronyms

R&D	Research and Development.
PA	Polyamide.
PET	Polyethylene terephthalate.
RFL	Resorcinol formaldehyde latex.
DMA	Dynamic Mechanical Analysis.
TTS	Time Temperature Superposition.
MPT	MultiPurpose Testware.
MPE	MultiPurpose Elite.
CRBD	Completely randomized blocked design.
ANOVA	Analysis of Variance.
DIN	Deutsches Institut für Normung.

1 Introduction

1.1 Continental AG

Continental was founded in Hannover in 1871 as the stock corporation "Continental-Caoutchouc- und Gutta-Percha Compagnie". Manufacturing at the main factory in Hannover included soft rubber products, rubberized fabrics, and solid tyres for carriages and bicycles.[1]

As of 2016, Continental employed more than 220 000 people, operating at 427 locations in 56 countries.[2] This global corporation has shown commitment in innovation and progress for over 145 years while developing technologies, systems, and service solutions that make mobility and transport more sustainable, safer, more comfortable, more customised, and more affordable.[3]

Today, as a developer and supplier of brake systems, systems and components for powertrains and chassis, instrumentation, infotainment solutions, vehicle electronics, tyres and technical elastomers, Continental contributes to enhanced driving safety and global climate protection.[1]

1.2 Motivation and contributions of the work

Hysteresis is, according to current literature, the main contributor to rolling resistance in the tyre, which in turn leads to energy losses, increasing fuel consumption.

The study of the hysteretic properties of textile reinforcements allows for a better understanding of its impact on the tyre performance and provides valuable information on what configurations provide better results, allowing optimisation in future tyre development.

The main contribution of this work was the development of a test method that would allow the determination and evaluation of these properties in textile reinforcements.

In addition, several studies were carried out, using the developed procedure, in order to evaluate the effect of testing parameters such as temperature and frequency, as well as cord dependent parameters such as twist, linear density and dip pick up percentage.

1.3 Organization of the thesis

This master's thesis is divided into 7 sections. The purpose of each one of these sections is described as follows:

- Section 1 - *Introduction* exposes an overview of the developed work and its importance to Continental AG.
- Section 2 - *Context and state of the art* presents the current knowledge on the modern tyre, textile reinforcements, and rolling resistance, as well as a brief introduction to viscoelasticity and hysteresis.
- Section 3 - *Technical description* describes the equipment and testing methodology used in this study.
- Section 4 - *Results and discussion* includes a display of the obtained results and their analysis.
- Section 5 - *Conclusion* presents a brief review of the results and the main conclusions of the thesis.
- Section 6 - *Assessment of the work done* consists of a critical analysis of the developed work, mentioning achieved goals and suggestions for further study.
- *References* is a complete list of all the sources referred throughout the thesis.

2 Context and state of the art

2.1 Overview of the modern tyre

The *tyre* is a complex technical component of today's motor cars and must perform a variety of functions. It must cushion, dampen, assure good directional stability, and provide long-term service.[4]

Most important of all, however, it must be capable of transmitting strong longitudinal and lateral forces (during braking, accelerating and cornering manoeuvres) in order to assure optimal and reliable roadholding quality. It must be able to do all of this even when the road provides little traction in wet or slippery conditions or when the road is covered with snow or ice.[4]

A high-tech tyre must be as balanced as possible in all of its characteristics.[4] Optimisation of a single aspect should not be achieved without considering the effect on all other properties and overall performance.

2.2 Materials used in a tyre

The components of a modern radial tyre for passenger cars contain diverse ingredients in differing amounts. These ingredients vary by tyre size and type. The typically used materials are listed as follows and an example of their distribution is shown in Figure 1.[4]

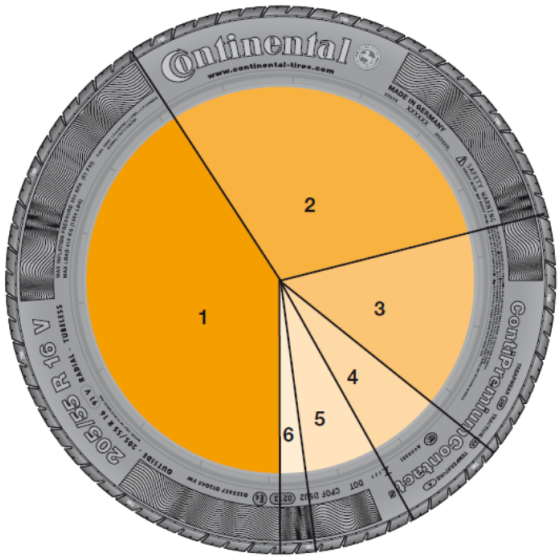


Figure 1: Breakdown of ingredients from a summer tyre.[4]

1. *Rubber* (natural and synthetic rubber) - 41 %.
2. *Fillers* (carbon black, silica, chalk, etc) - 30 %.
3. *Reinforcing materials* (steel, polyester, rayon, nylon, aramid) - 15 %.
4. *Plasticisers* (oils and resins) - 6 %.
5. *Chemicals for vulcanisation* (sulphur, zinc oxide, various other chemicals) - 6 %.
6. *Anti-ageing agents* and other chemicals - 2 %.

2.3 Tyre components

A modern tyre is made up of different components as shown in Figure 2 and explained as follows.[4]



Figure 2: Tyre structure.[5]

Tread/Belt assembly, consisting of:

1. *Tread* - Made of synthetic and natural rubber, it ensures high mileage, good road grip and water expulsion and comprises three components:
   - *Cap* - Provides grip on all road surfaces, wear-resistance and directional stability.

- *Base* - Reduces rolling resistance and damage to the casing.
- *Shoulder* - Forms an optimal transition from the tread to the sidewall.

2. *Jointless cap plies* - Made of nylon, embedded in rubber, these enable high speeds.
3. *Steel cord belt plies* - High-strength steel cords that allow optimisation of directional stability and rolling resistance, increasing the tyre's mileage performance.

Casing/Carcass, consisting of:

4. *Textile cord ply* - Made of rayon or polyester (rubberised), it controls internal pressure and maintains the tyre's shape.
5. *Inner liner* (below textile cord ply) - Made of butyl rubber, its function is to make the tyre airtight.
6. *Sidewall* - Made of natural rubber, it protects the casing from external damage and atmospheric conditions.
7. *Bead reinforcement* - Promotes directional stability and precise steering response and is made of nylon and aramid.
8. *Bead apex* - Made of synthetic rubber, it promotes directional stability, steering performance and comfort level.
9. *Bead core* - Consisting of steel wire embedded in rubber, it ensures firm seating of the tyre on the rim.

2.4 Textile reinforcements

A tyre's reinforcing elements are predominant load-carrying components. They provide strength and stability to the sidewall and tread as well as contain the air pressure.[6] As with all tyre components, the choice of a reinforcement cord for a given application may require compromises involving cost, intended market segment and end-use application.[7]

Currently, four materials make up the major tyre *textile reinforcement* usage: rayon, nylon, polyester, and aramid.[7]

2.4.1 Rayon

Rayon is a cord made from regenerated cellulose produced by wet spinning.[6] The low-shrink, high-modulus, good-adhesion properties of rayon make it an excellent choice for use in passenger tyres. However, rayon has lost market share to polyester due to higher cost and environmental concerns with production facilities.[7]

Advantages: Stable dimensions; heat resistant; good handling characteristics.
Disadvantages: Expensive; sensitive to moisture; environmental manufacturing issues.[6]

2.4.2 Nylon

Nylon (PA) is a generic term for aliphatic polyamides. Two varieties are used in tyre cords: Nylon 6 (polycaprolactam) and Nylon 6.6 (product of adipic acid/hexamethylene diamine condensation).[7] Nylon tyre cords are synthetic long-chain polymers produced by continuous polymerization/spinning or melt spinning.[6]

Advantages: Good heat resistance and strength; less sensitive to moisture.
Disadvantages: Heat set occurs during cooling (flat-spotting); long-term service growth.[6]

2.4.3 Polyester

Polyester tyre cords are also synthetic, long chain polymers produced by continuous polymerization/spinning or melt spinning.[6] Polyethylene terephthalate (PET), the most common polymer of the polyester family, is the condensation polymerization product of ethylene glycol and terephthalic acid.[7]

Advantages: High strength with low shrinkage and low service growth; low heat set; low cost.
Disadvantages: Not as heat resistant as nylon or rayon.[6]

2.4.4 Aramid

Aramid is a synthetic, high tenacity organic fibre produced by solvent spinning. It is 2 to 3 times stronger than polyester and nylon.[6] Aramid is a wholly aromatic polyamide. The

most common commercial material is poly(p-phenylene terephthalamide), e.g., Kevlar™ or Twaron™. Aramid cords have very high strength, high modulus, and low elongation. The relatively high cost has slowed adoption where other cheaper materials are performing well.[7]

Advantages: Very high strength and stiffness; heat resistant.
Disadvantages: Cost; processing constraints (difficult to cut).[6]

2.4.5 Hybrid

Design and production of *hybrid cords* is a simple and economical way of modifying the physical properties to obtain a new generation of tyre cords.[8] These hybrid cords are made by blending dissimilar yarns,[9] allowing the combination of properties from two different materials into a single cord.

2.5 Cord design

The terminology used for defining tyre reinforcements comes from the textile industry.[7] As such, an overview of key terms and concepts is presented to allow a better understanding of the design and properties of textile reinforcements.

Regarding cord components and characteristics:

Filament: the smallest continuous element of a cord.[7]
Yarn (or thread): a coherent length of filaments laid (or plied) together.[10,11]
Cord: a twisted or formed structure composed of two or more yarns.
Titer: the linear density defined as the mass in grams per length; typically in dtex (= g / 10,000 meters).
Twist level: the number of turns per unit length of a yarn or cord; typically in turns per meter (tpm).
Twist direction: it is termed "S" if the spiral turns clockwise from top to bottom for a vertically held cord and "Z" for a similar counterclockwise turning.[7]
Cord construction: it is typically specified as the polymer decitex followed by the ply number.

Endless multifilament yarns are used for the construction of tyre reinforcement cords. These may have a different linear density and twist level, according to their material and final application.

Regarding the fibre's properties:

Strength: the tensile load required to rupture a cord at a given rate of extension, i.e., the breaking load of a given cord.[7]
Tenacity: a measure of the strength of a fibre, quoted as strength per linear density.[10]

Regarding the processing:

Spinning: the process by which filaments are assembled into yarns.
Twisting: imparting twist to a single yarn or the twisting of several single yarns together to obtain a cord.[10]
Weaving: the operation by which cords are woven together into a fabric.[7]
Dipping: a treatment of the textile, typically using a resorcinol formaldehyde latex (RFL) based coating; this process creates an interface that allows the bonding between the cord and the rubber, improving the adhesion; often, an epoxy coating is used in order to increase the compatibility between the cord surface and the RFL coating.[12]
Calendering: the technique by which the textile and the rubber are combined; it is also known as rubberisation.[10]

Of particular importance to this study are the twisting and the dipping. An important parameter is the twist factor (TF), which correlates the twist level and the titer, as shown in Equation 1.

$$\mathrm{TF} = \textit{Twist level} \times \sqrt{\frac{\textit{Total cord dtex}}{10000}} \tag{1}$$

The content of dip in the cord is quantified as dip pick up (DPU) percentage, which corresponds to the weight percentage of dip on the cord, following Equation 2, in which M_d is the mass of the dip and M_dc is the mass of the dipped cord.[13]

$$\mathrm{DPU} = \frac{M_\mathrm{d}}{M_\mathrm{dc} - M_\mathrm{d}} \times 100 \tag{2}$$

2.6 Rolling resistance

The future sustainability of road transportation will require substantial improvement in the efficient use of energy by road vehicles.[14]

The pneumatic rubber tyre is a dominant solution in the automotive sector, due to its reliability and effectiveness in meeting the wide diverse driving functions and requirements of vehicles under various road conditions, which makes it unparalleled in the market. However, there are some areas that still need further improvements. One area, that is attracting a lot of attention and concern, due to its importance and impact, is the tyre's rolling resistance.[14]

Rolling resistance can be perceived as the mechanical energy loss of the tyre as heat, because of tyre rolling for a given distance.[14]

In general, the rolling resistance occurrence is undesirable to both vehicle performance and environmental welfare. It is found to be one of the main factors opposing the vehicle's mobility, particularly at higher velocities, and leads to energy losses; making the vehicle consume more fuel to maintain its mobility.[14]

According to the current literature, the tyre's rolling resistance is due to three mechanisms:[14]

- The *tyre's cyclic deformation* which causes some losses in its internal mechanical energy (i.e. strain energy loss). This is due to several occurrences such as the components' friction and their viscoelastic properties. Among these occurrences, hysteresis damping holds the dominant impact, being responsible for about 80–95 % of the total tyre's rolling resistance.

- The *aerodynamic drag*, due to the tyre cutting through the surrounding air as it rotates, which opposes tyre movement and promotes heat transfer between the air and the tyre. Such phenomenon can cause 0–15 % of the total tyre's rolling resistance depending on the tyre speed.

- The *frictional slip* that takes place when the tyre comes into contact with the wheel rim and with the road surface during its rotation which leads to heat build-up. This is the least important causal factor, accounting for about only 5 % of the total tyre rolling resistance.

Regardless, the rolling resistance is not entirely bad as its existence, to some degree, is necessary to achieve other essential functions like good tyre grip, traction, cornering and braking.[14]

Thus a target conflict arises, making it necessary to explore solutions that aim to decrease rolling resistance, and therefore fuel consumption, without disregarding its effect on road adhesion and grip.

Nonetheless, many studies reveal that the tyre's rolling resistance can be responsible for up to approximately 20–30 % of the vehicle's total fuel consumption.[14]

As such, an increase for tyre research and development for low rolling resistance has been noted, with focus on the main source, i.e. hysteresis damping. This research has explored three design aspects of the tyre: the structure and body construction, the dimensional features, and the materials.[14]

Current literature's focus is on seeking low hysteresis rubber materials. As such, compound and cord rubber composites properties and their effect on hysteresis have been extensively studied and documented.[14,15] However, the properties of textile reinforcements and their impact in viscoelastic and hysteretic behaviour have not yet been substantially studied. To the knowledge of the author, only a few articles on the subject are available.[16–18]

As such, the study of the hysteresis properties of cord reinforcements, as a function of parameters such as temperature, frequency, amplitude, decitex and twist level, can be valuable in order to allow further tyre improvement.

2.7 Hysteresis

2.7.1 Elasticity and viscoelasticity

Strain is typically defined as the ratio between the change in length and the original length of a sample, as represented in Equation 3. *Stress* corresponds to the load applied to a sample, adjusted for the geometry of the specimen, using the cross-sectional area, as demonstrated in Equation 4.[19]

$$\varepsilon = \frac{\Delta l}{l} \tag{3}$$

$$\sigma = \frac{F}{A} \tag{4}$$

Different materials show different strain responses to an applied stress.

Perfect *elastic* materials possess an ideal linear stress-strain characteristic.[20] Elastic deformation is instantaneous, which means that total deformation occurs the instant the stress is applied or released (i.e., the strain is independent of time). In addition, upon release of the external stress, the deformation is totally recovered - the specimen assumes

its original dimensions.[21] For an applied load as shown in Figure 3(a), this behaviour is represented in Figure 3(b).

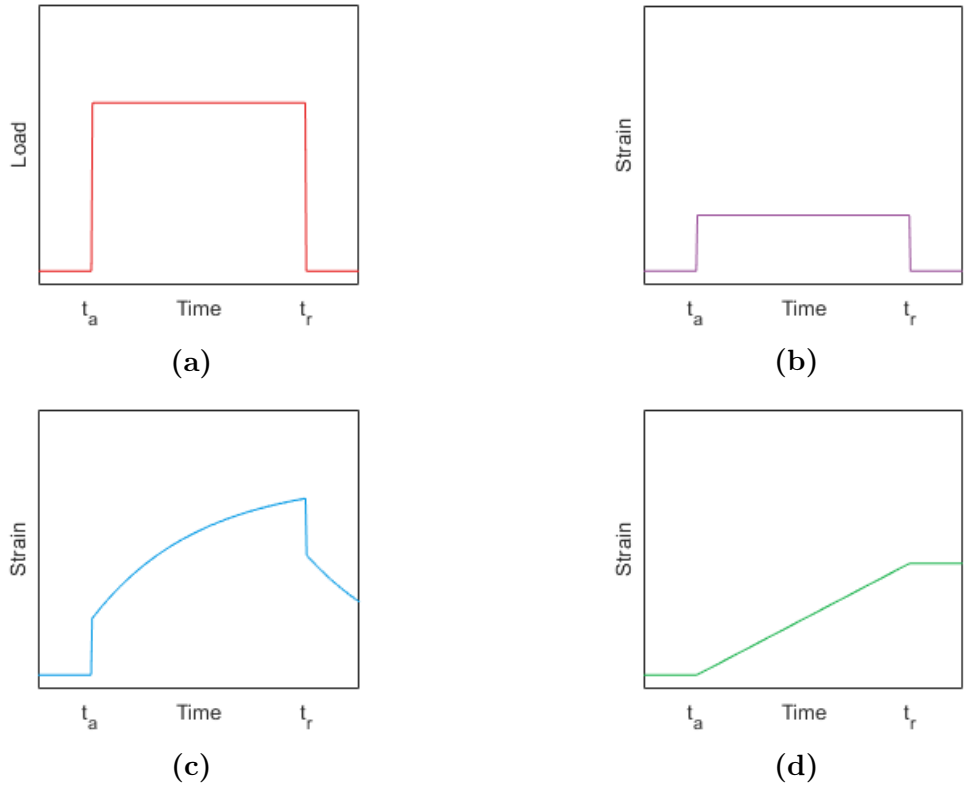


Figure 3: Elastic (b), viscoelastic (c), and viscous (d) response to a load applied at time t_a and released at t_r (a).[21]

By way of contrast, a purely *viscous* material shows the phenomenon called anelasticity;[22] that is, in response to an applied stress, deformation is delayed or dependent on time. Also, this deformation is not reversible or completely recovered after the stress is released.[21] This phenomenon is demonstrated in Figure 3(d).

For the intermediate *viscoelastic* behaviour, the imposition of a stress in the manner of Figure 3(a) results in an instantaneous elastic strain, which is followed by a viscous, time-dependent strain.[21] This behaviour is illustrated in Figure 3(c).

Polymers, such as the previously mentioned textile reinforcement materials, show viscoelastic behaviour - that is, characteristics intermediate between elastic and viscous behaviour.[22]

Another way of differentiating these materials is through their stress-strain curves. Figure 4(a) shows the stress-strain curve of an ideal elastic material. The load and unload curves are the same, and the energy lost as heat per cycle is zero in this case. In practice, there

is always a viscous component present. As such, the unload curve does not, in fact, follow the load curve. The shaded area in Figure 4(b) is a representation of the dissipated energy in each cycle.[22] The shape obtained is known as the *hysteresis* loop.[20]



(a) **(b)**

Figure 4: Stress-strain plot for elastic (a) and viscoelastic (b) behaviour.[22]

2.7.2 Dynamic Mechanical Analysis

Dynamic Mechanical Analysis (DMA) is a technique that uses dynamic perturbations to study a material's response to stress, temperature, frequency and other parameters.[19]

In order to characterize the viscoelastic behaviour of a material, the material is sinusoidally deformed, and the resulting stress is recorded.[22] For an ideal elastic material, the stress and strain are in phase, as shown in Figure 5, and the phase shift is $\delta = 0°$. For an ideal viscous material, the stress and strain are 90° out of phase (i.e., $\delta = 90°$). However, a viscoelastic behaviour is more common. Figure 6 shows a viscoelastic response with a phase lag between the stress and the strain.[22]

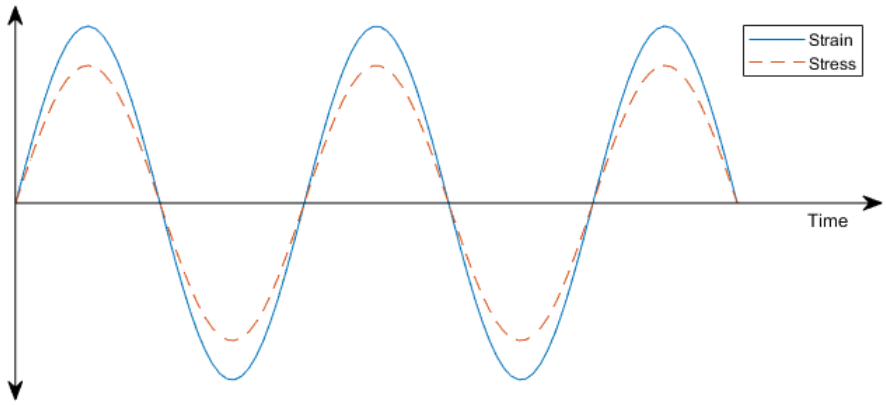


Figure 5: Stress and strain over time for a purely elastic material.[22]

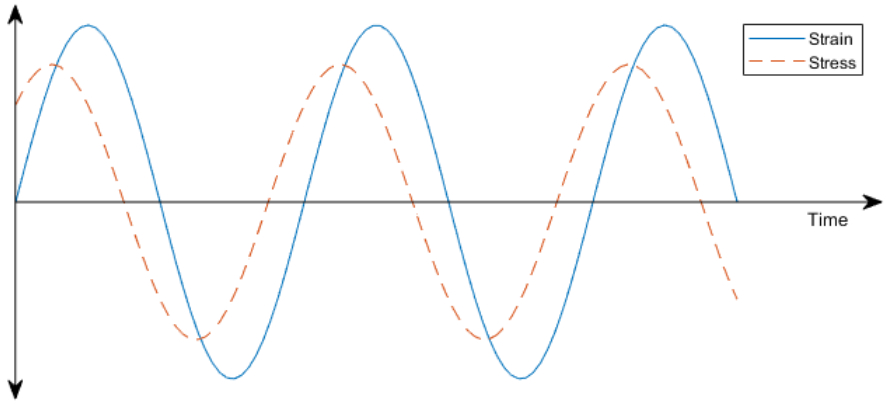


Figure 6: Stress and strain over time for a viscoelastic material.[22]

The material is subjected to an oscillatory strain with frequency ω.[22] The following expressions describe strain and stress:

$$\varepsilon = \varepsilon_0 \sin(\omega t) \tag{5}$$

$$\sigma = \sigma_0 \sin(\omega t + \delta) \tag{6}$$

In Equation 6, δ is the phase angle or phase lag between the stress and strain.[22] From these expressions, two moduli are defined:

$$E' = \left(\frac{\sigma_0}{\varepsilon_0}\right) \cos\delta \tag{7}$$

$$E'' = \left(\frac{\sigma_0}{\varepsilon_0}\right) \sin\delta \tag{8}$$

E' is known as the *storage modulus* and E'' as the *loss modulus*.[22]

Alternatively, using complex variables:

$$\varepsilon = \varepsilon_0 \exp(i(\omega t)) \tag{9}$$

$$\sigma = \sigma_0 \exp(i(\omega t + \delta)) \tag{10}$$

$$E = \frac{\sigma}{\varepsilon} = \left(\frac{\sigma_0}{\varepsilon_0}\right) \exp i\,\delta = \left(\frac{\sigma_0}{\varepsilon_0}\right) (\cos\delta + i \sin\delta) = E' + iE'' \tag{11}$$

Figure 7 shows the graphical relationship between these variables. The storage modulus is a measure of the stored energy, i.e., the elastic part, while the loss modulus is a measure of the energy lost as heat, i.e., the viscous part.[22]

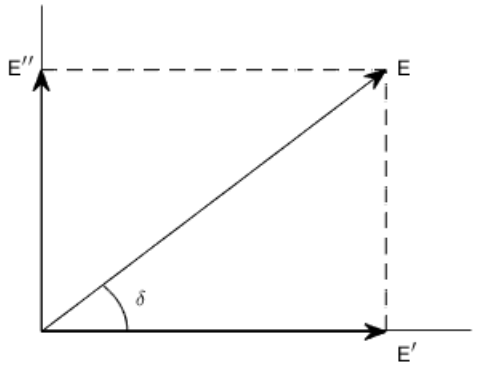


Figure 7: Vectorial representation of the complex modulus.[22]

These two moduli can be defined in terms of the phase shift:

$$E' = E \cos\delta \tag{12}$$

$$E'' = E \sin\delta \tag{13}$$

A new term called the *loss factor* can now be defined as follows:

$$\text{Loss factor} = \tan\delta = \frac{E''}{E'} \tag{14}$$

This term is proportional to the ratio of the maximum energy dissipated per cycle to the maximum energy stored in the cycle.[22]

The evaluation of these variables will be valuable to describe the viscoelastic and hysteresis behaviour of the reinforcement materials studied in this thesis.

3 Technical description

The objective of this project was to study the influence of certain parameters in the mechanical properties of textile reinforcement cords, focusing on the hysteretic behaviour. The DMA technique was used in order to study the effect of parameters such as temperature, frequency, linear density, twist and DPU %.

3.1 Test system and basic procedure

The tests were performed using an MTS Acumen 3 Test System (Figure 8) connected to an MTS Flextest 40 Controller and combined with the MultiPurpose Testware (MPT) and Elite (MPE) applications. A Mytron KPK 27 KH Climate Chamber was used in order to control temperature and humidity during the tests. This configuration allows the creation and operation of an automated and customized test procedure, as well as the acquiring of the data throughout the test.



Figure 8: MTS Acumen 3 Test System.[23]

A typical test preparation started with the clamping of the sample, assuring an initial sample length (l_0) of 100 mm. All samples were previously kept in a controlled environment, at 23 °C and with 55 % humidity, and were only carried to the laboratory at the time of testing.
The test procedure itself began with a ramp to a hold value of the applied load, typically known as pretension. This value is always 0.05 cN/dtex and is based on nominal titer (which corresponds to the linear density in dtex multiplied by the ply number). After this, the displacement is offset, ensuring a standardization of the samples.
This is followed by an initial sample conditioning which consisted of 10 cycles, at reduced

velocity, from a low to a relatively high displacement, in order to pre-damage the sample and to exclude this effect from the dynamic response. These steps are followed by a ramp to a mean displacement value, after which this value is held for a certain amount of time, to assure the stabilization of the applied force.
The next step is the dynamic portion, consisting of the application of a sinusoidal deformation at a certain frequency and with a certain amplitude of the initial sample length.

This type of procedure allowed the dynamic characterization of the samples, by the monitoring of properties such as E', E'' and $\tan\delta$, following DIN Specification 53513.[24]

The maximum frequency used for testing was 30 Hz, as mechanical resonance could be observed for higher values, which would corrupt the measurement accuracy of the force transducer.[25] The minimum frequency used for testing was 1 Hz since it was determined that the load cell's resolution would not allow for lower frequencies, as the response and the noise of the transducer became comparable.

The internal temperature of a passenger car tyre under normal use usually lies between 20 and 60 °C when travelling. This value is also dependent on the type of tyre, the way the car is driven, and the ambient temperature.[26] In the design of the experiments, temperatures included in the service range were preferred, in order to focus on the expected behaviour of the cords.

3.2 Testing and data analysis

The developed work in this thesis can be divided into four sections.

The first section comprises an initial *setup optimisation*, which consisted mainly of changes in the clamping system, in order to decrease variation between replicates.

The second section consists of a study developed to analyse the variation of the hysteretic properties in nylon cords as a function of their *linear density and twist*.

The third section corresponds to the development of a test method and subsequent optimisation, in order to construct a *master curve*. This will allow the Time-Temperature Superposition principle to be proven or refuted when applied to textile cords.

The final section is focused on the determination of the influence of the *DPU %* in the dynamical mechanical properties of polyester cords.

3.2.1 Setup optimisation

The first test results using the DMA technique showed an unexpected amount of variation between replicates. Considering this is a previously unused technique, both for textile reinforcements and using the MTS test system, before establishing a definitive test procedure, some basic tests were performed in order to verify if the clamping was the source of the results' low reproducibility. Tensile tests were performed using Nylon 6.6 cords with a 940×2 construction, at 23 and 100 °C, in order to determine if slippage of the specimen was occurring.

Following this, 3 types of clamping setups were considered:

1. The initial setup, combining a set of mechanical parallel clamps, as in Figure 9(a), and an ordinary wrench to close them.

2. The same mechanical clamps but using a torque wrench, shown in Figure 9(b), for the tightening.

3. Pneumatic parallel clamps, similar to the one shown in Figure 9(c).



(a) **(b)** **(c)**

Figure 9: Tested clamping setups, where (a) corresponds to the initial setup,[27] (b) shows the torque wrench added for the second setup,[28] and (c) shows the pneumatic clamp.[29]

After determining which configuration showed better results and easier handling, its performance was optimised by testing different inlays. An inlay consists of a piece of material that is placed in the clamping surface in order to protect the sample from damage. Materials such as sandpaper, tape, and two types of aluminium alloy were tested and compared to the reference setup, without inlay.

Lastly, the chosen setup was tested at different temperatures to verify the improvement and to guarantee its proper functioning.

3.2.2 Linear density and twist study

To evaluate the influence of the linear density and the twist in the viscoelastic behaviour of cords, a two-factor three-level experimental design was proposed. Nylon 6.6 cords with a by two (×2) configuration and with characteristics as described in Table 3 were constructed for the purpose of this study.

Table 3: Cord characteristics for the linear density and twist study.

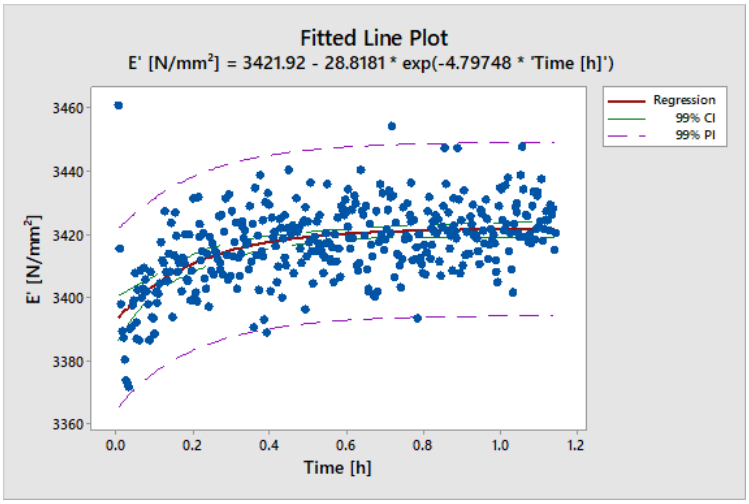
Sample	Linear Density [dtex]	Twist Level	Twist Level [tpm]	Twist Factor
1	470	Low	250	77
2		Medium	420	129
3		High	600	184
4	940	Low	231	100
5		Medium	350	152
6		High	461	200
7	1400	Low	170	90
8		Medium	290	153
9		High	378	200

The medium twist values correspond to the typical production specifications for the respective cord construction.
In a reasonable range (between 100 and 600 tpm), values for a lower and higher twist were chosen, in order to obtain an even spread, as much as possible. Unfortunately, the 470×2 cord with a high twist (Sample 3) was impossible to produce.

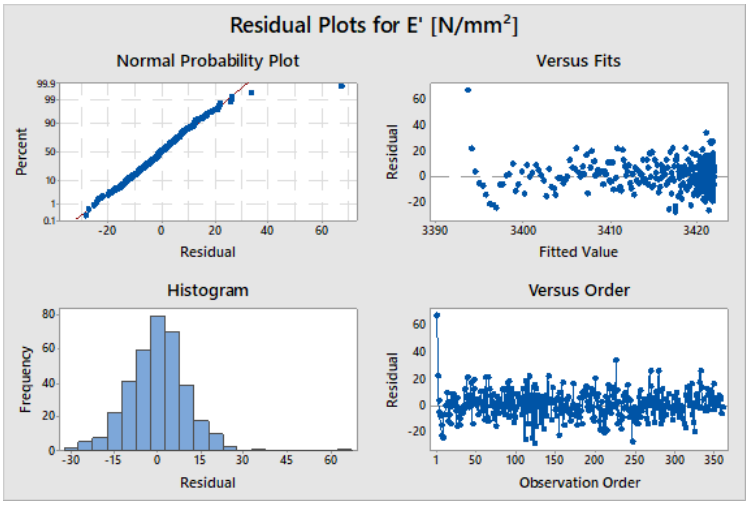
For these samples, 1 h tests were determined to be sufficient to obtain response data that showed a clear trend over time (t), for E', E'' and $\tan\delta$. This response data was fit to an asymptotic regression, using Minitab 17, as exemplified in Figure 10(a). The function used, displayed in Equation 15, provided not only a good fit, as shown in Figure 10(b), but also allowed the prediction of a steady state value, assuming the limit as time approaches infinity, as presented in Equation 16.

$$y = \theta_1 - \theta_2 \exp(-\theta_3 \times t) \tag{15}$$

$$\lim_{t\to\infty} y = \theta_1 \tag{16}$$



(a)



(b)

Figure 10: Example of the non linear regression of the data, where (a) corresponds to the fit and (b) to the analysis of the residuals.

These tests were performed at 23 °C and at 55 % humidity, with 10 pre-damaging cycles, at 120 mm/min, from 1 to 8 % displacement. The selected mean displacement was of 5 %, with a dwell period of 5 minutes. The dynamic test was conducted at 10 Hz, with a ±1 % amplitude. This study, with 5 replicates per combination, added up to a total of 40 runs.

In addition to the dynamic tests, standard tensile tests (5 replicates per sample) were performed on the cords described in Table 3, in order to observe the pre-existing difference between them in static mode. This evaluation was especially focused on the applied mean strain of 5 %.

3.2.3 Master curve construction

The mechanical behaviour of viscoelastic materials depends on frequency and temperature. In general, there is an equivalence between the frequency and temperature behaviour during relaxation processes.
This phenomenon is known as the Time-Temperature Superposition (TTS) principle. This principle can be applied to construct a master curve at a reference temperature from a series of isothermal frequency sweeps. These frequency sweeps are performed in a range directly accessible to the DMA instrument. Curves measured at temperatures below the reference are shifted horizontally to higher frequencies so that the end segments of the obtained curves overlap to the greatest possible extent. In the same way, curves measured at higher temperatures are shifted to lower frequencies. An illustration of this procedure is shown in Figure 11. Thus, a master curve describes the mechanical properties of polymers covering a frequency range wider than that accessible by direct measurement.[30]

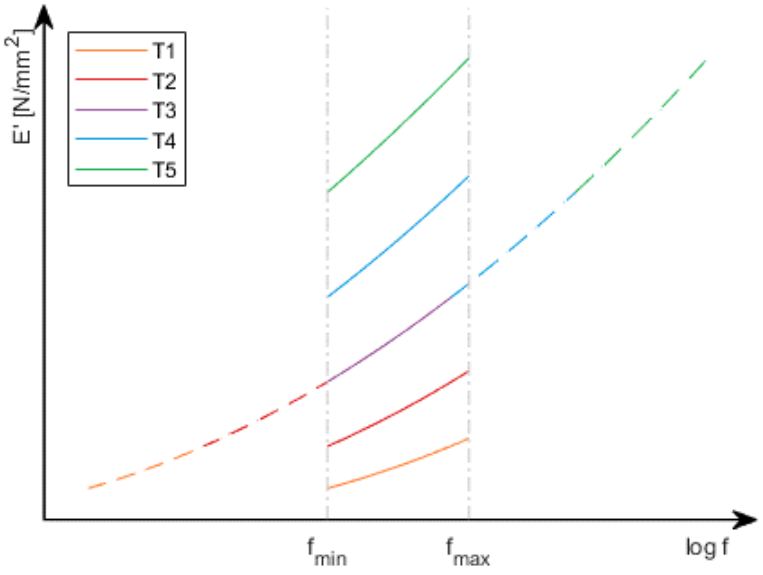


Figure 11: Construction of a master curve (dashed line), from isothermal frequency sweeps (full line), in which T1 > T2 > T3 > T4 > T5.

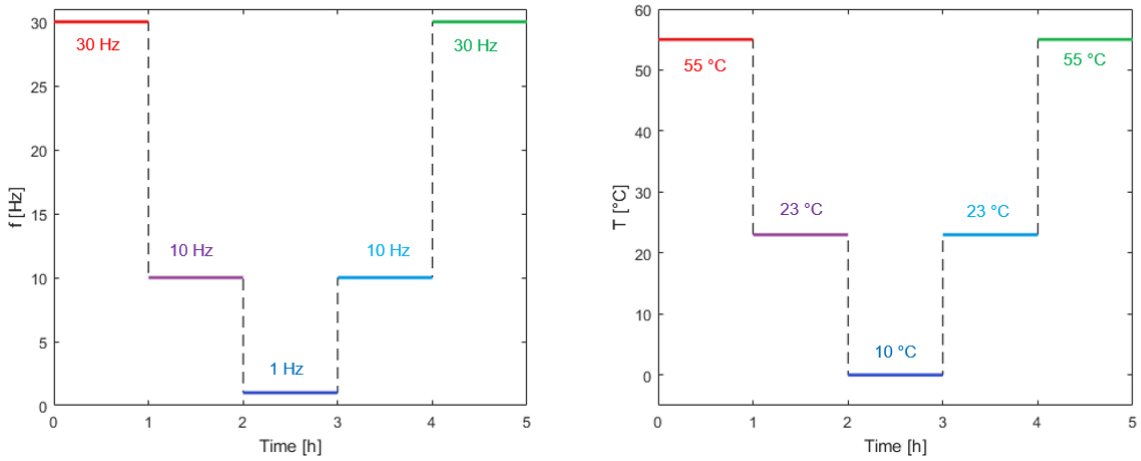
For this project, the main objective was to define a testing procedure that would allow the acquiring of accurate and reproducible dynamic results at different frequencies and temperatures, while maintaining a reduced testing time.

In order to obtain an initial idea of how factors such as temperature, frequency, testing time and history affected the samples, two types of test were devised:

1. A test composed of 5 blocks, each with a duration of 1 h, with a change in frequency

by steps, following 30 Hz → 10 Hz → 1 Hz → 10 Hz → 30 Hz. This was performed at 23 °C on a fresh sample of Nylon 940×2. An illustration of the procedure is given in Figure 12(a).

2. A similar procedure, at a constant frequency of 10 Hz, with varying temperature by steps, following 55 °C → 23 °C → 0 °C → 23 °C → 55 °C, as represented in Figure 12(b).



(a) **(b)**

Figure 12: Illustration of the test procedure by frequency (a) and temperature (b) steps.

Besides determining which variation approach is more suitable, this test was considered in order to establish if starting with the most extreme setting allowed for a better conditioning of the cord, decreasing the necessary testing time for the subsequent blocks, as proposed in literature.[31]

After this initial evaluation, the test procedure proposal consisted of frequency sweeps nested in a temperature sweep. Hence, equally distributed frequency values in a logarithmic scale were chosen between 1 and 30 Hz, while the temperature values were selected between -20 and 160 °C, limited by the climate chamber's capacity, with a $\Delta T = 20$ °C.

The primary concept consisted of starting at the most extreme setting, for both frequency and temperature. From here and maintaining the initial temperature, testing at first frequency was set to last for 2 h, followed by 20 min per block for each subsequent frequency. At the end of this frequency sweep, the temperature would be decreased to the following level, at which a similar frequency sweep would be carried out. This process is illustrated for the first three temperatures in Figure 13.

A second concept involved an identical procedure, but starting from the lowest tempera-

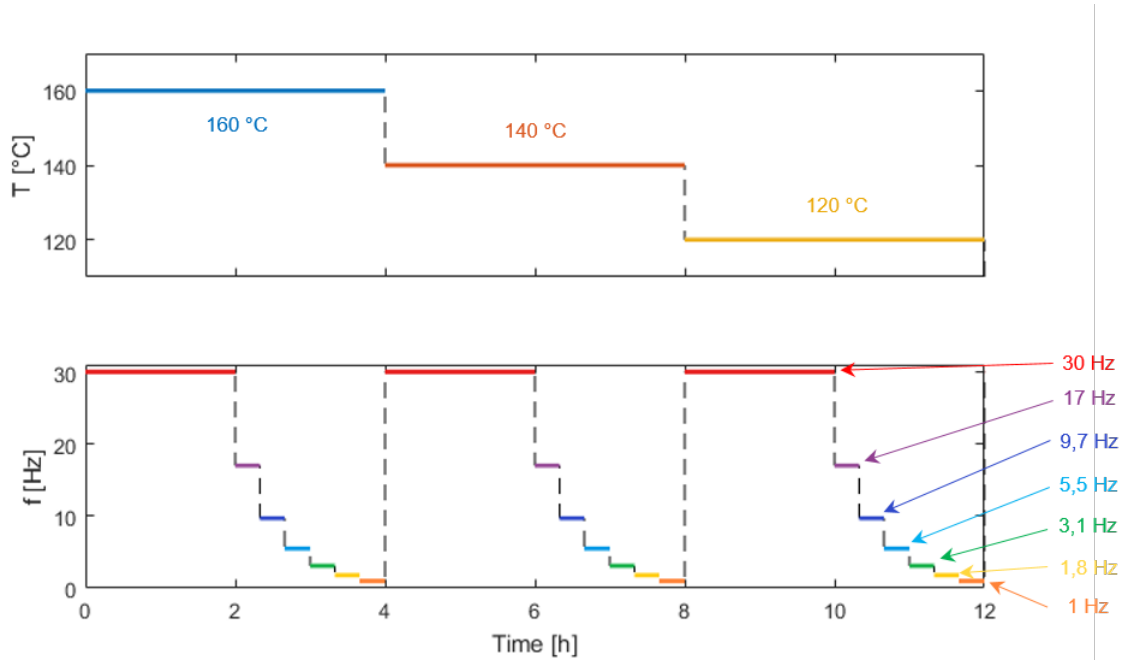


Figure 13: Illustration of the nested frequency sweeps in a temperature sweep procedure, with decreasing temperature steps.

ture and rising up to 160 °C. The frequency sweeps however were executed in the same manner.

As a comparison point, equal frequency sweeps were carried out using fresh samples for two single temperatures, 0 and 100 °C.

The test with increasing temperature steps was the only one from which a complete sweep could be obtained. As such, each section of data, obtained via this procedure, was fitted using a similar approach to that shown in Figure 10. This allowed the prediction of a limit value for E', E'' and $\tan\delta$, with respect to each combination of temperature and frequency. These values were used in order to construct a master curve and determine the shift factor (a_T) function.

The master curve is constructed by shifting the obtained isothermal frequency sweep curves around a reference temperature, by applying the following transformation, for all three variables:

$$y(\omega, T) = y(\omega \cdot a_T, T_{ref}) \tag{17}$$

For the testing temperatures, each individual value of a_T was determined manually, by attempting to visually obtain a smooth looking curve for E'. This allowed the fitting of the shift function, which corresponds to a_T as a function of temperature, whose parameters are valuable for future cord behaviour simulation.

3.2.4 DPU % study

To evaluate the influence of the dip pick up percentage (DPU %) in the hysteretic behaviour of cords, a completely randomized blocked design (CRBD) was proposed. PET cords with variable DPU % were used to study the influence of this parameter. The description of these samples is shown in Table 4.

Table 4: Cord characteristics for the DPU % study.

Sample	Material and Construction	DPU %
1	PET 2200 x 2	3.43
2		4.95
3		6.57

For these samples, 16 h tests were determined to be sufficient to obtain response data that showed a clear trend over time, for E', E'' and $\tan\delta$. The data, excluding the first 4 h, was fit to an asymptotic regression, in a similar way to the fitting procedure used for the linear density and twist study. These tests were also performed at 23 °C and at 55 % humidity, with 10 pre-damaging cycles, at 120 mm/min, from 1 to 8 % displacement. However, the mean displacement value was of 6 %, in order to avoid buckling of the cord. The dwell period was of 30 min, as the PET showed a slower stabilization of the applied force. The dynamic test was conducted at 10 Hz, with a ± 1 % amplitude. For this study, with 3 replicates per combination, a total of 9 runs were carried out.

In addition to the dynamic tests, the samples described in Table 4 were subjected to microscopic analysis of cross-sectional cuts, in order to observe the penetration of the dip.

4 Results and discussion

The results presented in this section are divided into four parts following those previously described in Subsection 3.2.

4.1 Setup optimisation

Tensile tests were performed at two different temperatures, 23 and 100 °C, in order to determine if slippage of the cord was in fact occurring. These tests consist in a controlled increase of tension until the breaking point. For each condition, 5 samples were tested. The obtained force-elongation curves are represented in Figures 14 and 15.

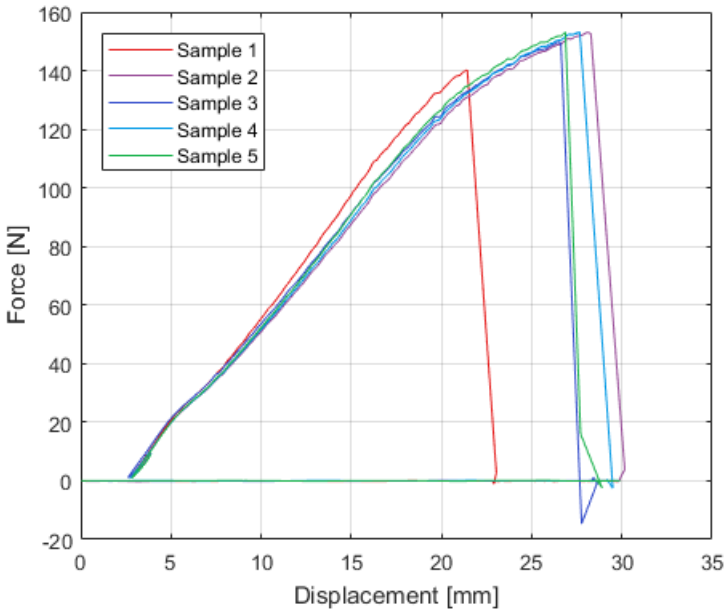


Figure 14: Force-elongation curves for Nylon 6.6 with a 940×2 construction, at 23 °C.

Analysing Figure 14 closely, some noise can be noticed for higher values of displacement, which is indicative of a successive slippage of the cord in very small amounts, especially under higher tensions. The considerable difference between Sample 1 and the other replicates may also be attributed to that. However, given such small differences, slippage was the suspected cause but not an obvious one.
The test was also conducted at 100 °C, for which the softening of the cord and a decrease in viscosity of the dip was expected, increasing the extent to which the slippage occurred, as verified in Figure 15.

Slippage of the cord was thus confirmed for the initial clamping setup.

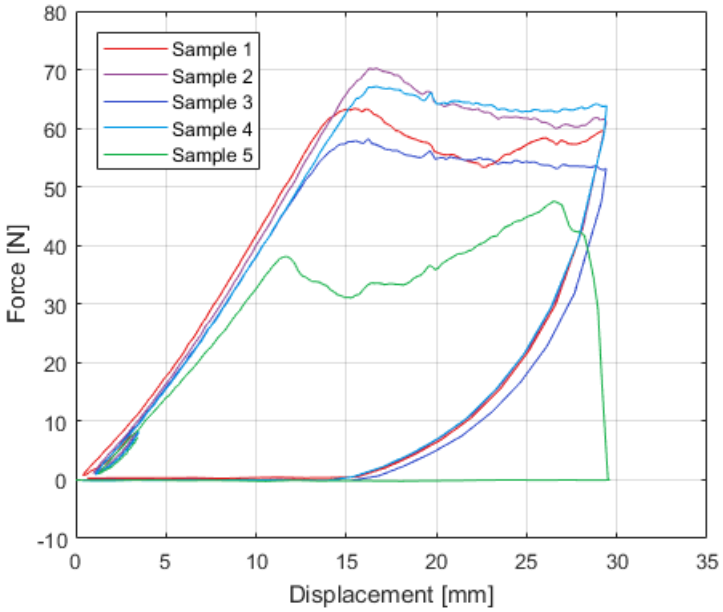


Figure 15: Force-elongation curves for Nylon 6.6 with a 940×2 construction, at 100 °C.

As described in Subsection 3.2.1, two other clamping configurations were considered, as they were expected to show the following improvements over the initial setup:

1. The initial setup allowed for slipping, resulted in different applied forces for each sample, as clamping was carried out without a reference; it also involved possible damage to the load cell since the action of the wrench caused the lower clamp to move.

2. The second setup, with the addition of the torque wrench, guaranteed the same applied torque for each sample at the beginning of the test, ideally decreasing variation between samples; however, it still allowed for possible slippage and it involved a similar risk of damage to the force transducer.

3. The last setup assured the same force was applied to all samples and kept throughout the test, minimizing slippage; the risk of damaging the load cell is avoided, as the clamping is pneumatically driven and controlled by means of a dual pedal switch.

In order to check the differences caused by the change in the clamping configuration, two samples were tested for each condition with the two new possible setups. The torque screwdriver was used to apply 5 or 10 N·m of torque, while the pneumatic clamps were tested using two pressures, 3 and 7 bar. For each condition, 2 samples were tested. The obtained force-elongation curves are represented in Figure 16.

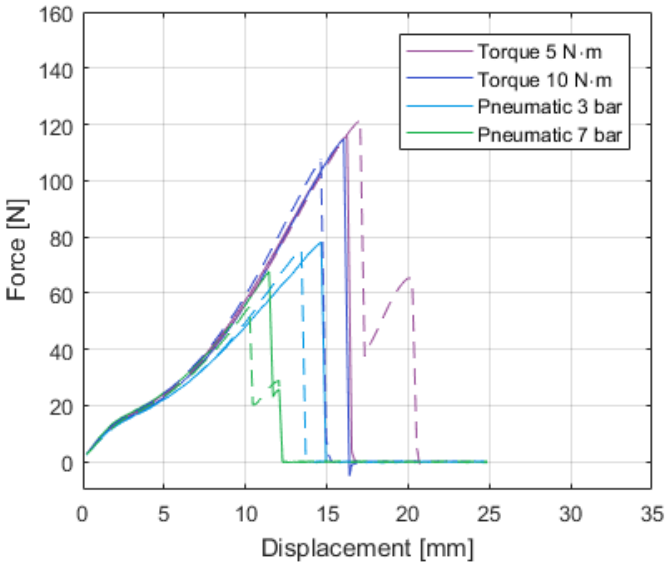


Figure 16: Force-elongation curves for Nylon 6.6 with a 940×2 construction, using the torque screwdriver or the pneumatic clamp setup.

Examining Figure 16, it is clear that a pressure of 3 bar, when using the pneumatic clamps, is not sufficient to avoid slippage. However, for all other configurations, the obtained results are satisfactory, as they follow the same path, with a very small variation between samples. Furthermore, the second setup seems to allow the cord to reach higher load and displacement values. This is likely due to differences in the surface of the clamps. The pneumatic grips that were used have a pyramidal clamping surface, which causes damage to the cord, leading to an early breaking point.
While a full comparison between Figures 14 and 16 isn't possible, considering the tests using the initial setup included a pre-conditioning of the sample, there is an obvious lack of shakiness observed in results of the second figure, supporting the conclusion of an improved configuration.

Given the adequate results of the pneumatic clamp setup at 7 bar and considering its advantages over the others in both handling and performance, additional tests were carried out using this system.

The testing of different inlays, in order to raise the breaking point of the cord, allowing a greater work range, was done using 2 samples for each condition. The results are presented in Figure 17.

For both sandpaper and tape, the inlay allows slippage of the cord, causing a clear deviation from the other curves, especially with tape.
However, both aluminium alloys ensure an improvement in the testing range, particu-

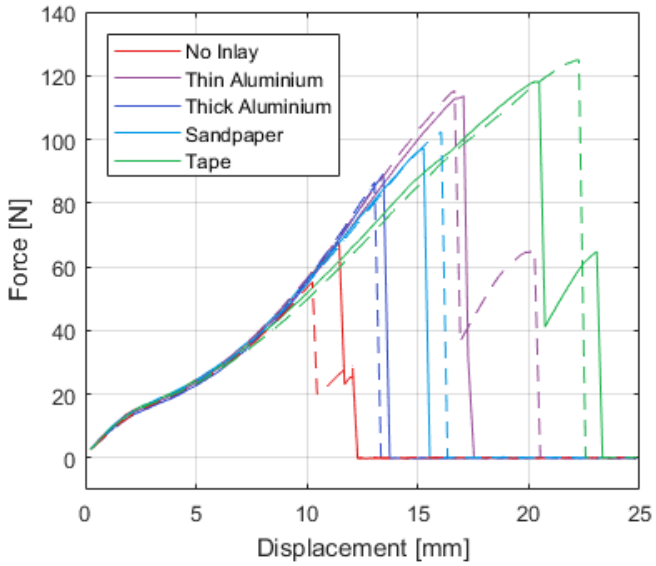


Figure 17: Force-elongation curves for Nylon 6.6 with a 940×2 construction, with respect to different inlays.

larly the thinner one. Given these results, a specifically constructed inlay, fittable and attachable to the clamping, was constructed out of the thicker aluminium alloy.

Lastly, to verify the applicability of this improved setup, tensile tests were carried out at three different temperatures, 23, 80 and 160 °C. Figure 18 shows the collected results, with 3 samples per condition.

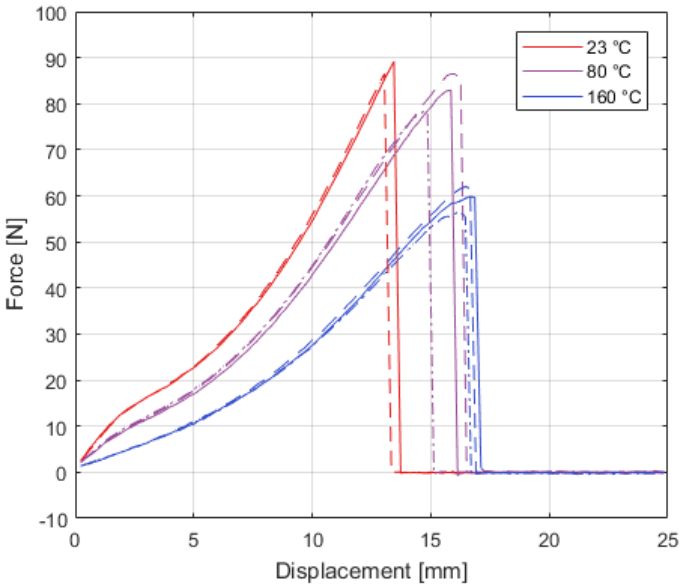


Figure 18: Force-elongation curves for Nylon 6.6 with a 940×2 construction, using the pneumatic clamps with an aluminium inlay, with respect to different temperatures.

While a slight variation increase is perceptible with increasing temperature, there is no indication of slippage even at higher temperatures. In addition, the expected softening of the cord with increasing temperature is observed.

Thus, the setup is considered optimised and the pneumatic clamping is used for all subsequent testing along with the aluminium inlay.

4.2 Linear density and twist study

Standard tensile tests, with 5 replicates per sample, were performed on the cords described in Table 3. The obtained mean force-elongation curves are represented in Figure 19.

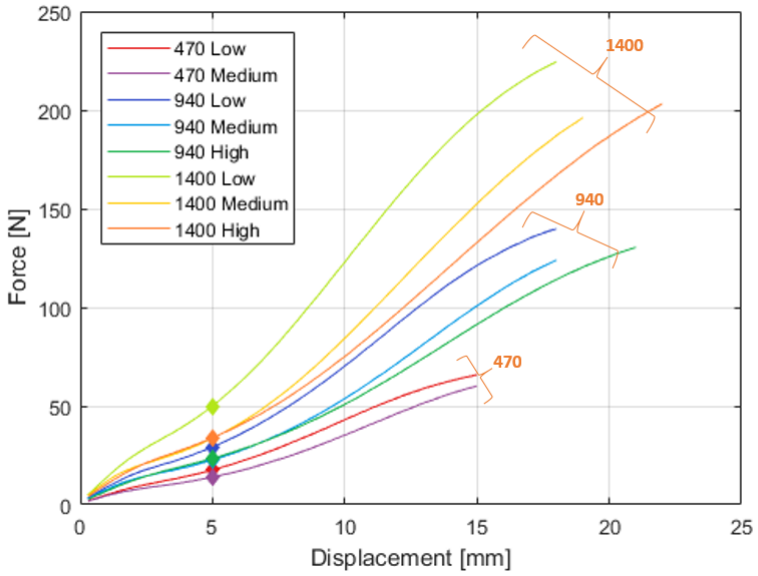


Figure 19: Force-elongation curves for Nylon 6.6 cords with variable twist and linear density.

The layered distribution of cords with the same linear density is particularly explicit, with higher force levels for higher linear density values. These results are expected as increasing dtex entails higher mass for samples of equal length.
The cord has two important contributions, the material and the structural component. As such, a cord will first go through a mainly structural elongation, followed by a section that consists mostly of material elongation. This behaviour agrees with the observed trend inside each linear density group, with lower twists requiring higher forces for the same displacement.
It is also noticeable that at a displacement of 5 %, the higher twist samples overlap with the medium twist ones. This can be explained due to a dominant structural component in this phase of the test.

The equivalent stress-strain curves are shown in Figure 20. In these, the force was normalized over the initial cross-sectional area of the cord, A_0, and the displacement over the initial length of the sample, l_0.

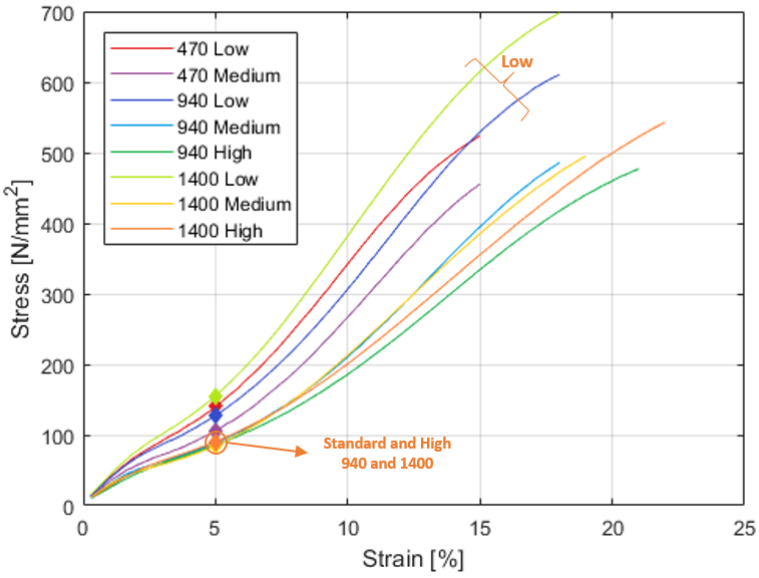


Figure 20: Stress-strain curves for Nylon 6.6 cords with variable twist and linear density.

A grouping of the lower twist cords is detected, requiring higher applied stress to reach the same strain. This can be explained due to the decreased packaging of the cords, entering the material component of the behaviour much earlier than the highly twisted cords.
A very interesting observation is that, for higher twist and linear density levels, the initial portion of the curves completely overlap. Again, this is a manifestation of the spring-like behaviour that the cord presents for lower strains, for which the structural component is overall dominant.

Concerning the dynamic testing, the determined steady-state values for E', E'' and $\tan\delta$ are graphically represented over twist and linear density in Figures 21 to 26.

Analysing Figures 21 and 22, both E' and E'' decrease linearly with increasing twist.

For the loss modulus, the slope of the trend seems rather constant independently from the linear density. However, for the storage modulus, some differences are suspected, which would indicate an interaction between twist and linear density. This could, however, be due to the fact that the variability of each group is not constant, possibly leading to a false assumption. Ways of overcoming this suspicion could be the increase of the number of replicates, approximating the distribution of each group to a normal one, and the increase of the testing range for twist, even though the current range covers the

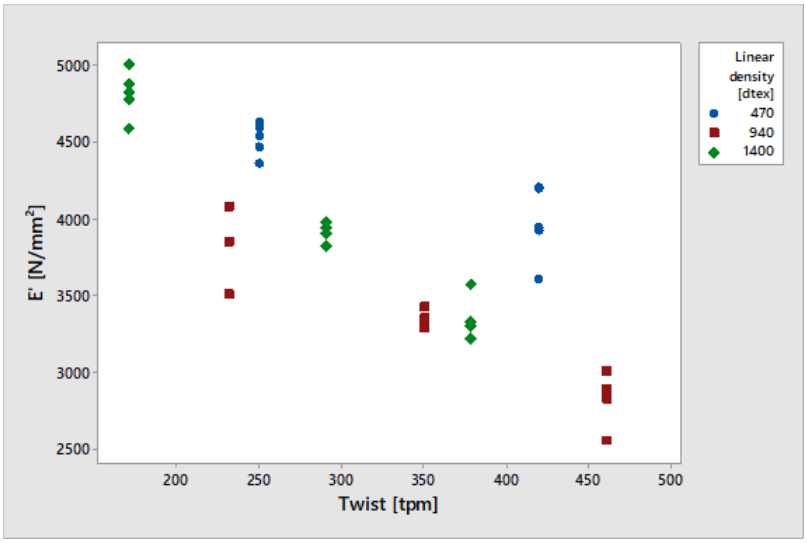


Figure 21: Scatterplot of E' over twist.

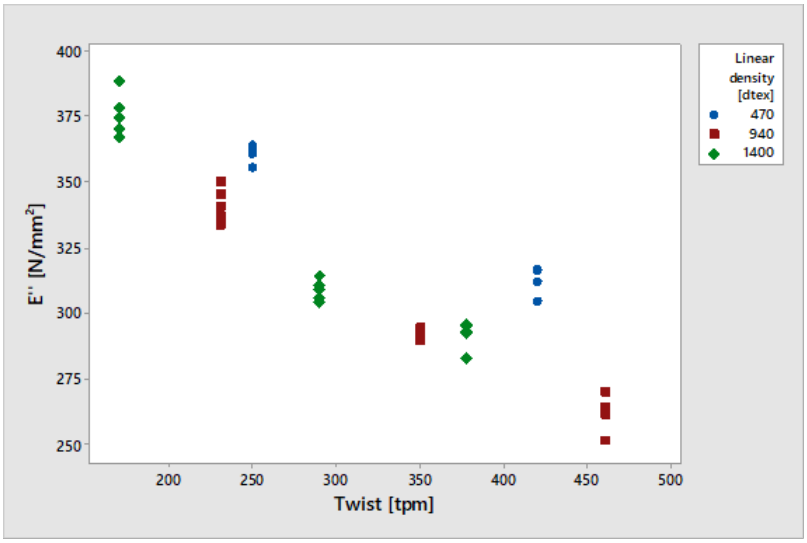


Figure 22: Scatterplot of E'' over twist.

values used for textile reinforcements. Nonetheless, this negative linear correlation over twist can be physically justified in a similar manner to the variations identified statically. For higher twists, a dominance of the structural component involves lower stresses for the same changes in strain. This happens because, as indicated by the results from the tensile tests, around an applied strain of 5 %, the cords with higher twists are still going through a process of uncoiling, which is permitted given the initial geometrical packaging of the cord. For lower twists, the cord, after reaching a fully structurally stretched conformation, is subject to the material elongation alone, leading to higher stress levels for the same changes in strain.

Another interesting finding corresponds to the impact that the twist variation has over E' and E''. A very small change in the number of turns per meter can impart a considerable variation in the dynamic properties of the cord. Comparing the extremes, an increase of around 300 tpm leads to a decrease of almost half the initial value of both E' and E''.

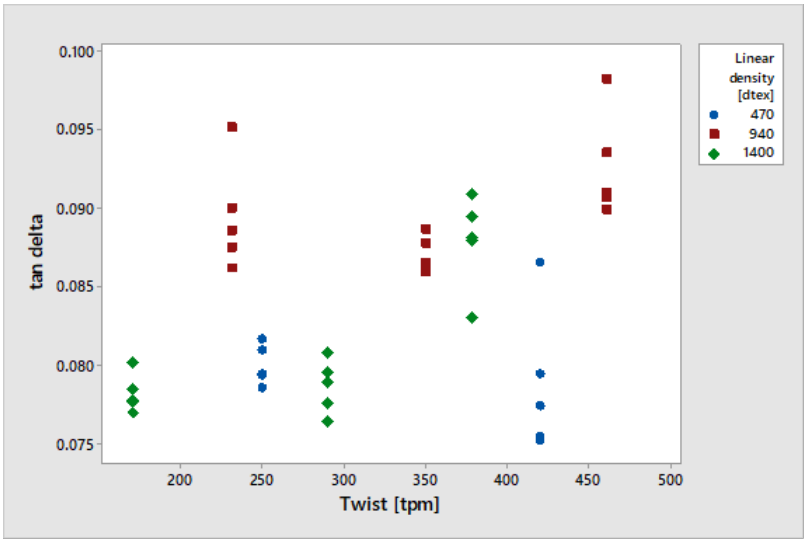


Figure 23: Scatterplot of $\tan\delta$ over twist.

Despite the observed variation for the storage and loss moduli, the obtained variation of the loss factor over twist is considerably small. A small increase of $\tan\delta$ is detected for the highest twist in the cords with 940 and 1400 dtex.
From Figure 23, it is already apparent that linear density seems to cause a more substantial variation, encountered when comparing the 940 dtex cords with the rest.

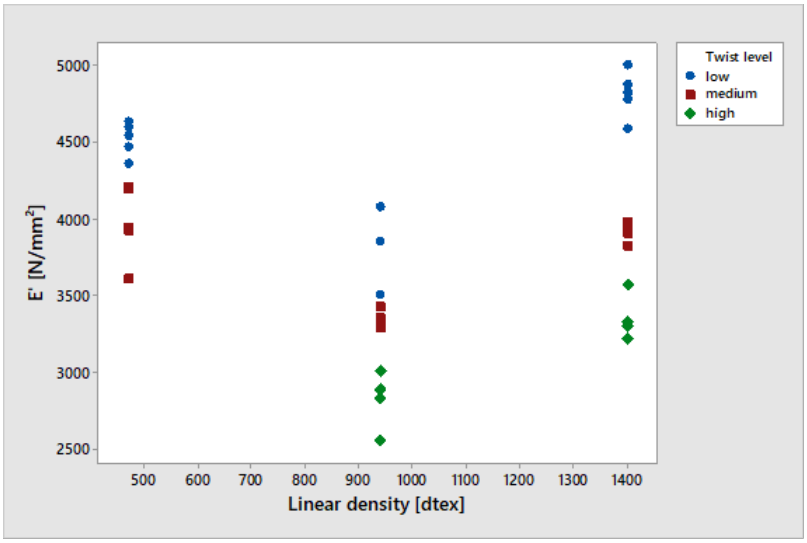


Figure 24: Scatterplot of E' over linear density.

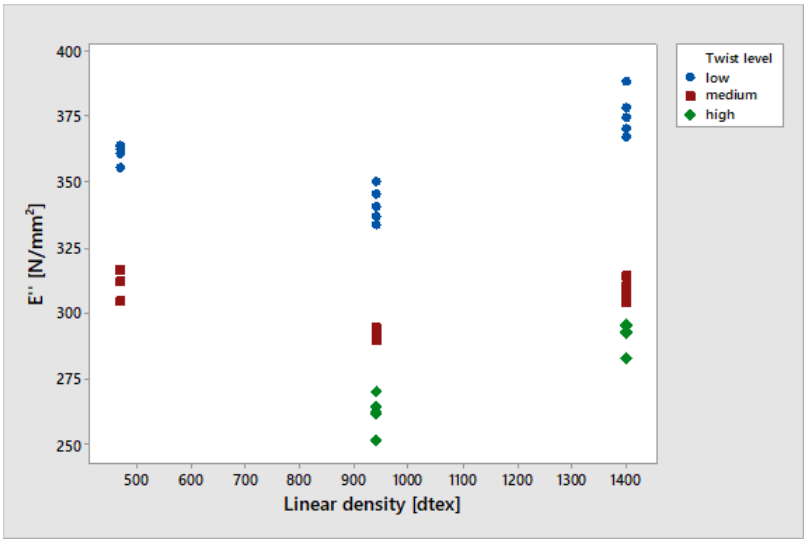


Figure 25: Scatterplot of E'' over linear density.

Analysing Figures 24, 25 and 26, the presence of curvature in the behaviour is evident, with the data points belonging to the 940 dtex cords showing proximity to the expected minimum for E' and E'', and maximum for $\tan\delta$. For the sake of clarity, while the twist values are not the same for each linear density level, they are grouped according to categorical twist levels.

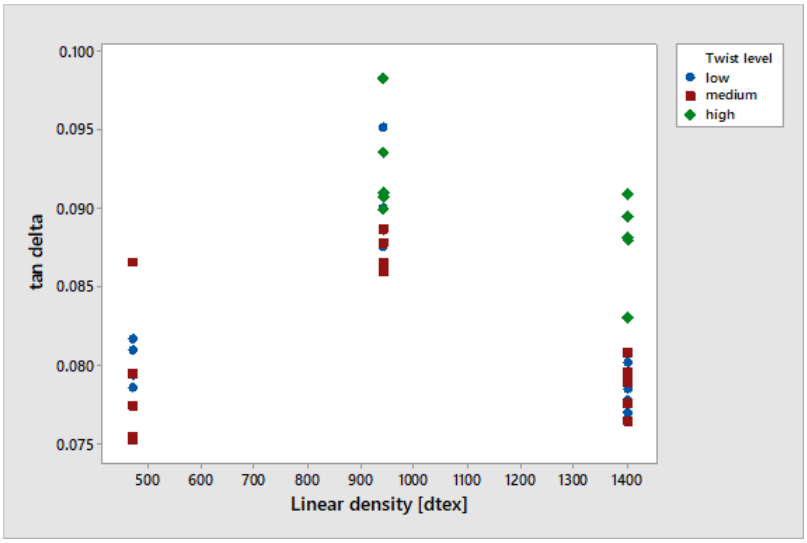


Figure 26: Scatterplot of $\tan\delta$ over linear density.

For the storage and the loss moduli, the linear density manifests less influence on the variation than that revealed with the twist, given that the data groups' intervals overlap each other to some extent.

However, for the loss factor, while the results for the lowest and highest level are quite

similar, the 940 dtex data shows an increase of almost 10 % over the response of the other two groups.

It has been found that the dipping process can impart not only an increase in the crystallinity degree of the cords but also a positive trend with increasing linear density, which is not observed for greige cords.[32]
Furthermore, an increase in linear density is accompanied by an increase in filament number and therefore in the contact area between yarns and filaments, increasing the friction when subjected to loading.
Both these hypothesis explain a positive linear correlation between the dynamic variables and linear density, which could translate into the observed behaviour between the groups with 940 and 1400 dtex. However, the physical reasoning behind the response of the lower level remains unascertained.
Possible approaches to this situation include:

- Further testing covering a wider range of linear density levels, in order to observe the actual trend and possibly detect deviations of these groups from it.
- Exploring the effects of the dipping process in the hysteretic properties of the cord, in order to identify a possible contribution to these results.

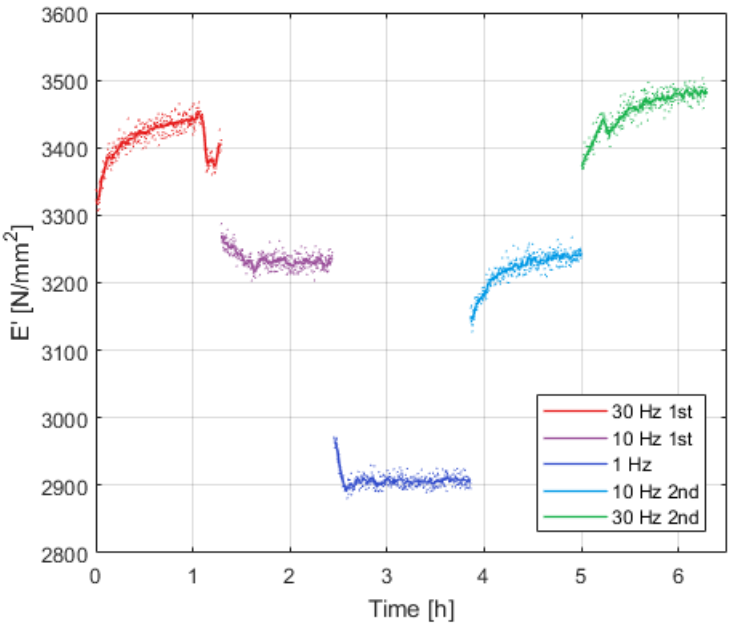
Nonetheless, with this study, it was possible to identify the degree of influence both twist and linear density have in the dynamical mechanical properties of Nylon 6.6 cords, as well as obtain an overall idea of the properties' values for the currently used textile reinforcements.

4.3 Master curve construction

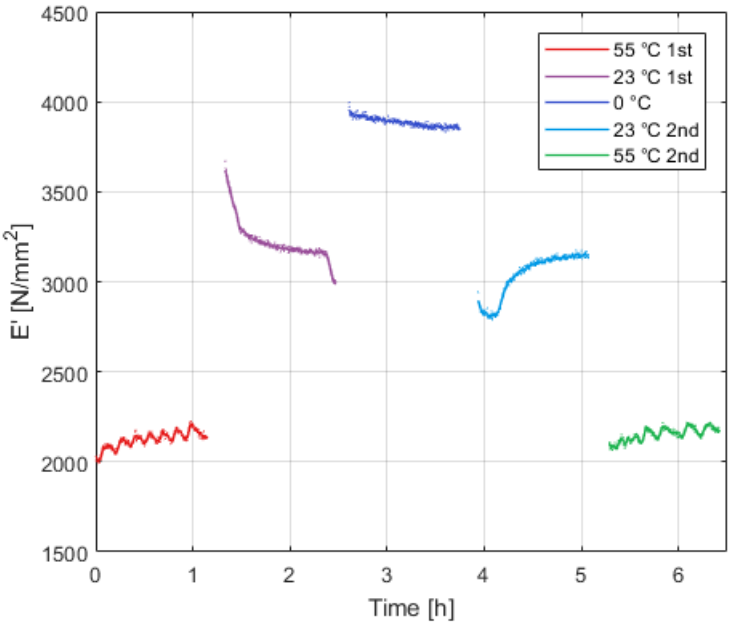
The initial experiments with varying frequency and temperature, as described in Subsection 3.2.3, were carried out by testing 2 samples for each procedure. The results are presented in Figure 27.

For this test procedure analysis, the storage modulus is used as representative of the results, as it shows more notable variations and similar conclusions can be drawn. The results for E'' and $\tan\delta$ are, however, available in Appendix B.

By examining Figure 27(a), which shows the results of the frequency based test, several conclusions can be drawn. As expected, a higher frequency corresponds to a higher value of E', as the material acts in a more elastic fashion, while at lower frequencies a more



(a)



(b)

Figure 27: Representation of E' for the frequency (a) and temperature (b) steps test procedure.

viscous or liquid-like behaviour is expected.[33]

Besides that, the first block, corresponding to the testing at 30 Hz, is the one with the most abrupt change, taking longer to stabilize or even get close to a limit value. The

following blocks, however, present a faster stabilization, taking less than 20 min to reach stable values for the lower frequencies. Thus, the initial more extreme setting works as a conditioning block, decreasing the necessary testing time for the following segments.
Furthermore, when repeating frequencies, the dynamic relaxation curve tends to the same limit values, from which one can conclude that the transient behaviour is reversible and the steady state is independent of the testing history.

Considering Figure 27(b), a similar behaviour is observed for temperature, as, for both 23 and 55 °C, the response tends to the same limit values.
Non surprisingly, these results present a lower modulus for higher temperatures, seeing as the material is softer and more fluid when heated.[33]
However, this approach shows a considerably higher variation between levels, which in turn translates into a longer waiting time for each condition, turning this strategy much less appealing when trying to decrease testing time.

In addition, an adaptation period seems to be necessary at 23 °C, in order to obtain the expected asymptotic behaviour. This might be due to the fact that the cord has to adjust to the temperature that is applied to the chamber. However, once the chamber is subjected to a temperature change, the frequency sweep only starts after the desired condition has been achieved in the chamber and after a waiting period of 5 min. The procedure was programmed in this way to assure that the cord is already at the desired temperature at the time of testing.

An extra test was run in the interest of determining if maintaining dynamic oscillation during the temperature change would cause any difference in the behaviour of the cord, as shown in Figure 28. As can be observed, the dashed lines, corresponding to the periods of change in temperature, lead to the same behaviour, seen in Figure 27(b), indicating that there are no significant implications from the non-application of an oscillatory deformation during the temperature change.

From these results, a test procedure based on achieving all conditions in a single test was proposed. To do so, frequency sweeps would be run from high to low frequencies at each temperature. In parallel, the temperature was changed at the end of each frequency sweep, as demonstrated in Figure 13.

The results of the four types of testing, described in Subsection 3.2.3, are shown in Figure 29. These results are adjusted over the time frame of the increasing temperature sweep (blue line) in order to allow comparison between the tests.
The initially proposed test, with decreasing temperature, showed some issues, as buckling

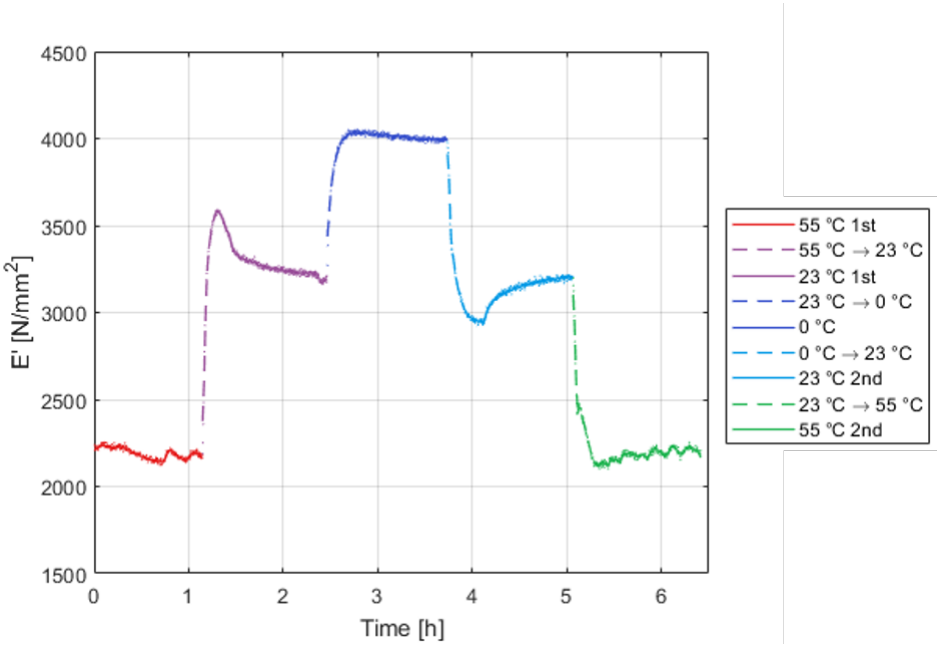


Figure 28: Representation of E' for the temperature steps test procedure, as a frequency of 10 Hz is maintained throughout the entire test.

of the cord was observed under 60 °C. As such, for lower temperatures, the obtained variable values were not valid and are not considered. Despite that, 2 samples were tested using this procedure, in order to evaluate the variability of the results. As can be perceived, when comparing the red and purple line, both samples showed a very similar behaviour with a constant difference between them. Seeing as this difference is maintained throughout the test, it was attributed to sampling variation.
The second attempt, with increasing temperature, from which the blue line was obtained, allowed the full procedure to be carried out.
Lastly, fresh samples were tested at 0 and 100 °C, obtaining the green and orange lines, respectively.

The procedure involving increasing temperatures was selected to provide the values for the master curve construction, as it produced results for all conditions in a reasonable amount of time. However certain differences were predicted and detected for this approach.
The initial approach allowed the cord to be stretched to a maximum length, with the first and highest temperature, which would be maintained throughout the test, enabling a consistent value for all conditions. However, this initial stretch worked as a contributor for the buckling effect observed at lower temperatures, seeing as, for these, the applied strain was too low to allow recovery, given the already imparted permanent deformation. In contrast, for the selected test, with each increasing temperature, the length of the specimen is suffering an adjustment to the newfound maximum length. This adds an unknown

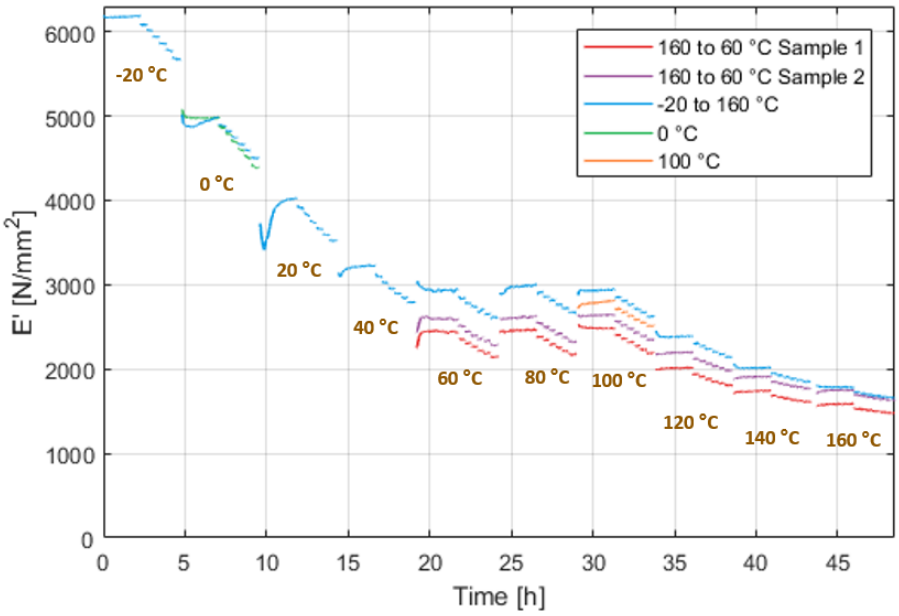


Figure 29: Comparative results for E' from the nested frequency sweeps in a temperature sweep procedures.

error to the obtained values, which cannot be corrected via the employed software.
This length difference justifies the slightly divergent trend the two approaches take when nearing lower temperatures, particularly visible in the 60 to 100 °C range.
When comparing the selected approach with the fresh sample tests it is clear that the difference is minimal and is contained within the expected sampling variation, from which one can conclude that no significant unexpected changes occur in the cord as a consequence of the extended testing time.
Given that there is no substitute method available that would grant better results, for now, the involved error was considered non-significant when evaluating the overall effect it would have in future simulation.

For each condition, from the selected test, the limit values were obtained using a similar fitting procedure to the one used for the twist and linear density study.

The fitted values over frequency are shown in Figure 30.
The data points corresponding to 30 Hz show an unusual behaviour, especially for E'' and $\tan\delta$, when compared to the rest of the trend, which might be due to previously undetected machine resonance at that frequency. As such, they were not used in the master curve construction.

As shown previously in Figure 11, the resulting isothermal frequency sweep curves were

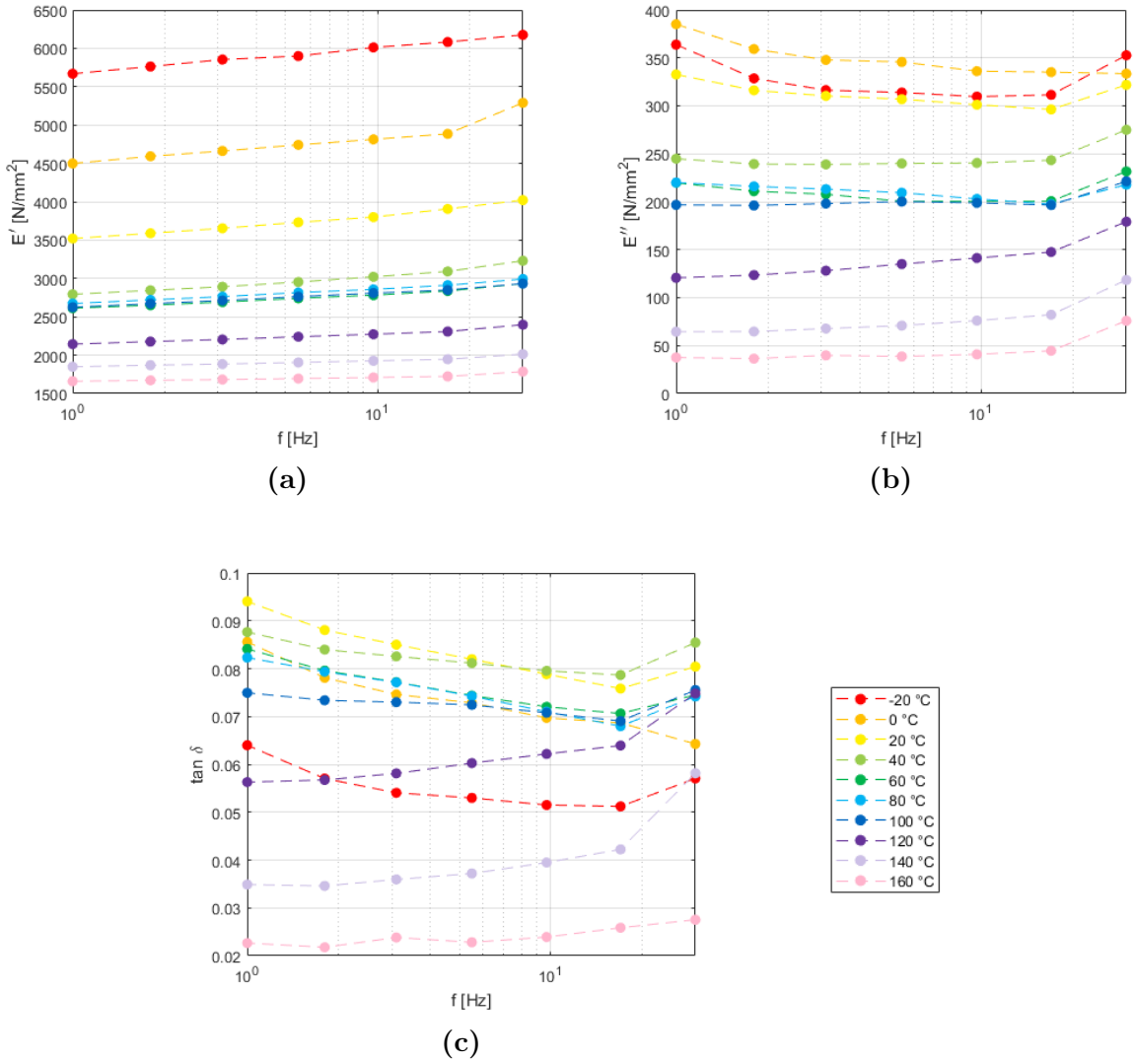


Figure 30: Plot of E' (a), E'' (b) and $\tan\delta$ (c) over frequency at different temperatures.

shifted in order to obtain a smooth looking master curve, as well as the corresponding shift factor function, which can be used in future projects. For confidentiality reasons, the obtained master curve and shift factor function are not disclosed in this document.

Additionally, the values presented in Figure 30, can be represented over temperature, resulting in Figure 31. In this figure, the viscoelastic properties' dependency on temperature is especially clear.
The decreasing trend of both E' and E'' with increasing temperature is observed, as expected with increasing softness of the material.
In addition, in the studied temperature range, two drops in E' are observed, from -20 to around 40 °C, and from 100 °C to the highest tested temperature. These drops are accompanied by peaks in both E'', at 0 and at 100 °C, respectively, and in $\tan\delta$, at around

20 and between 80 to 120 °C.

These variations can be justified by thermal transitions in the polymer, indicating how the molecular motions and free volume changes affect its behaviour.[34]

In fact, similar values have been described in literature, associating the first drop to a secondary transition, with increased segment mobility, and the second corresponding to the glass transition.[17] While the reported transition ranges are close to the detected ones, minor differences can also be justified by additional factors as, for example, differences in the level of crystallinity and in the cord construction.

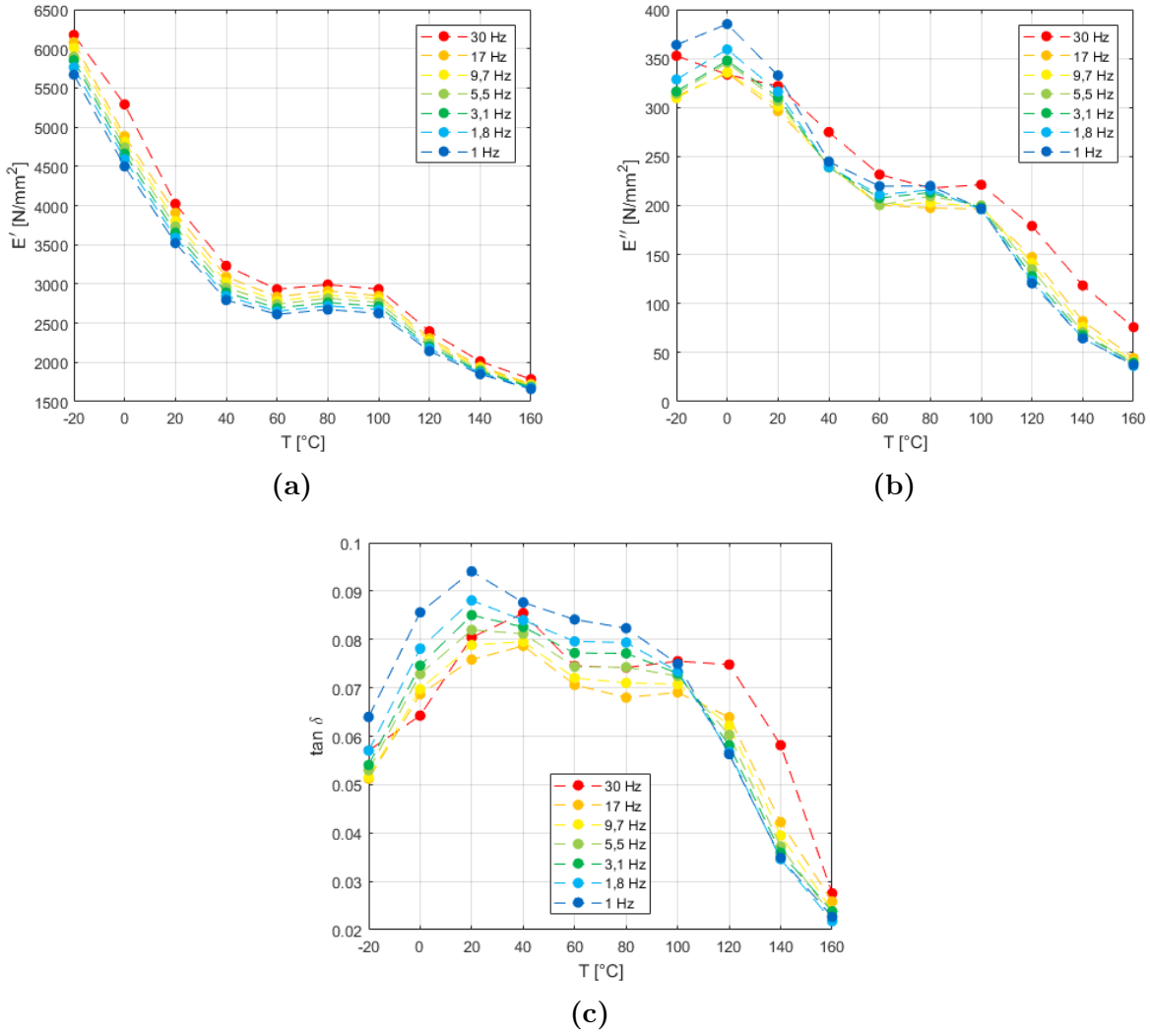


Figure 31: Plot of E' (a), E'' (b) and $\tan\delta$ (c) over temperature at different frequencies.

This study resulted in the development of a test procedure to examine the dynamic mechanical properties of textile reinforcements as a function of frequency and temperature. In addition, it provided valuable information in order to predict the hysteretic properties of cords when subjected to frequencies not accessible by direct measurement.

4.4 DPU % study

Regarding the dynamic testing, as mentioned in Subsection 3.2.4, the behaviour shown by PET required a much longer stabilization time in order to resemble an asymptotic behaviour. The first hours of the test also showed a much more significant change than that detected for Nylon 6.6. As such, in order to obtain a good fit and a better estimate of the limit value, the first four hours were not considered when fitting this behaviour. Given the extended testing time, only 3 replicates per condition were possible.

The determined limit values for E', E'' and $\tan\delta$ are graphically represented over DPU % in Figures 32, 33 and 34.
For E', as seen in Figure 32, a negative linear trend can be observed over the DPU %. However, the difference between the storage modulus values of each level is very small, not only considering the observed magnitude but also in comparison to the variation that was detected for Nylon 6.6 with linear density and twist.
For both E'' and $\tan\delta$ no particular trend is identified and, for all levels, the data ranges overlap each other, indicating that the loss modulus and factor are not greatly affected by the change in the DPU %.

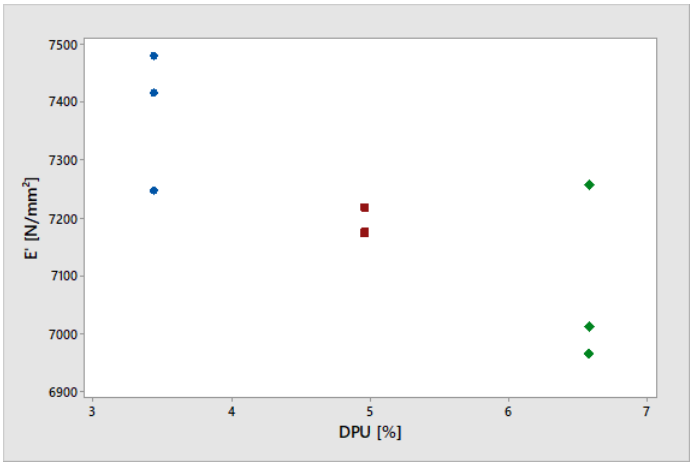


Figure 32: Scatterplot of E' over DPU %.

Using Minitab 17, a one-way ANOVA was performed for all three variables with DPU % as the factor, in order to check if there were significant differences between means. Equal variances were assumed for all groups, with a 95 % two-sided confidence interval.

The output tables of the performed ANOVAs can be found in Appendix C.

The DPU % showed a significant effect in E', with $F(2,6) = 5.29$ and $p = 0.047$, lower than the selected significance level, $\alpha = 0.05$.

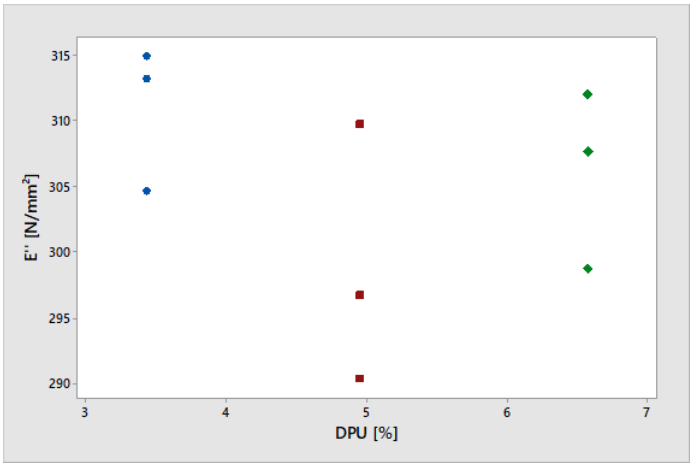


Figure 33: Scatterplot of E'' over DPU %.

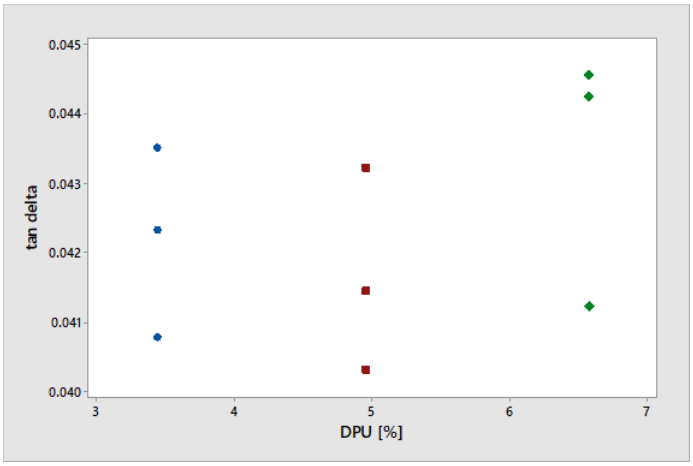


Figure 34: Scatterplot of $\tan\delta$ over DPU %.

The lower level showed a mean of 7380 N/mm^2 (StDev = 119) for E', while the higher levels showed respectively lower values, with a mean of 7188 N/mm^2 (StDev = 25) for 4.95 % and 7077 N/mm^2 (StDev = 119) for 6.57 %.
However, for both E'' and $\tan\delta$, the detected effect is statistically non-significant, as expected from the previously presented scatterplots, with both p-values > 0.05, respectively, $F(2, 6) = 1.87$, $p = 0.233$ and $F(2, 6) = 0.90$, $p = 0.456$.

As such, there is sufficient evidence that not all means are equal for the storage modulus, while for the other two variables, we fail to reject the null hypothesis.

In order to determine which groups differ from each other for E', a post hoc analysis using the Tukey pairwise comparison method was performed. The graphical representation is shown in Figure 35. Only the groups with 3.43 % and 6.57 % DPU present significant differences.

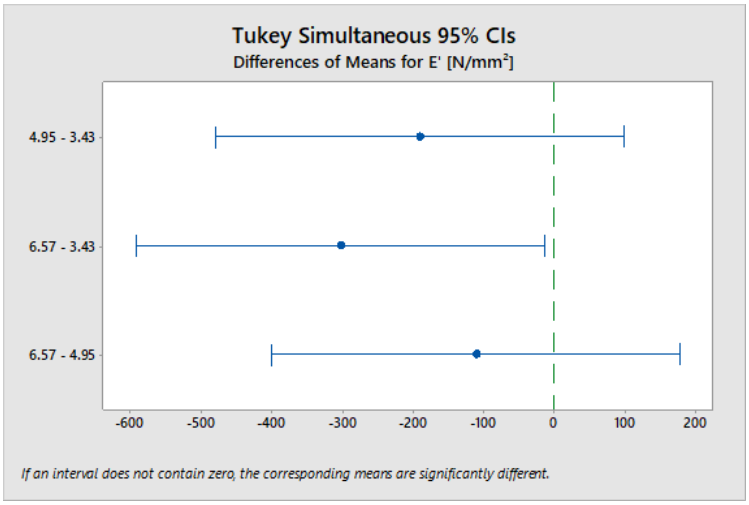


Figure 35: Graph of the Tukey comparison for E' over DPU %.

Lastly, a simple linear regression was carried out for this variable. The obtained fit is presented in Figure 36. The respective analysis of the residuals is presented in Figure 37.

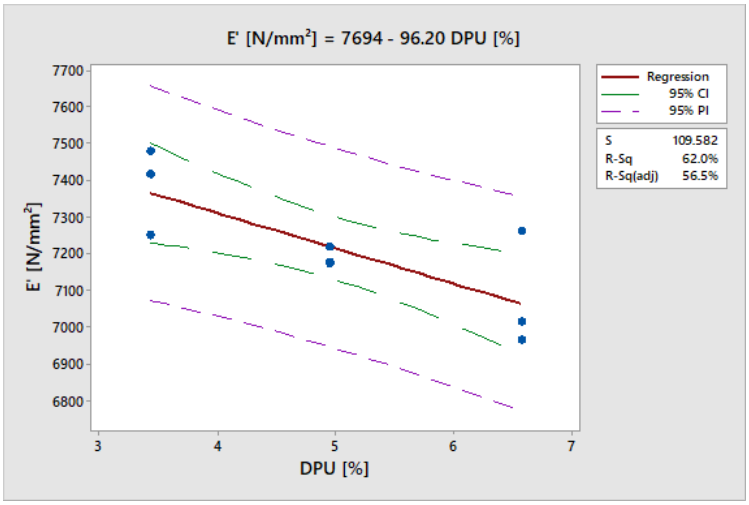


Figure 36: Linear regression fit for E' over DPU %.

The estimated model via the regression procedure is statistically significant, seeing as $p = 0.012 < 0.05$. The model shows an adequate fit to the data, with $p = 0.598 > 0.05$ for the lack-of-fit test. The obtained equation, E' [N/mm^2] $= 7694 - 96.2$ DPU [%], explains around 62 % of the variation in the data. However, one of the data points (Observation 2), belonging to the 6.57 % of DPU group, is considered an outlier, seeing as it presents a large residual and is not well fit by the equation.

From the residual plots in Figure 37, one can identify an apparently random pattern of residuals over the fitted values as well as over the order of observation. However, for such a small sample size, the normality is not clear, which is especially noticeable in the

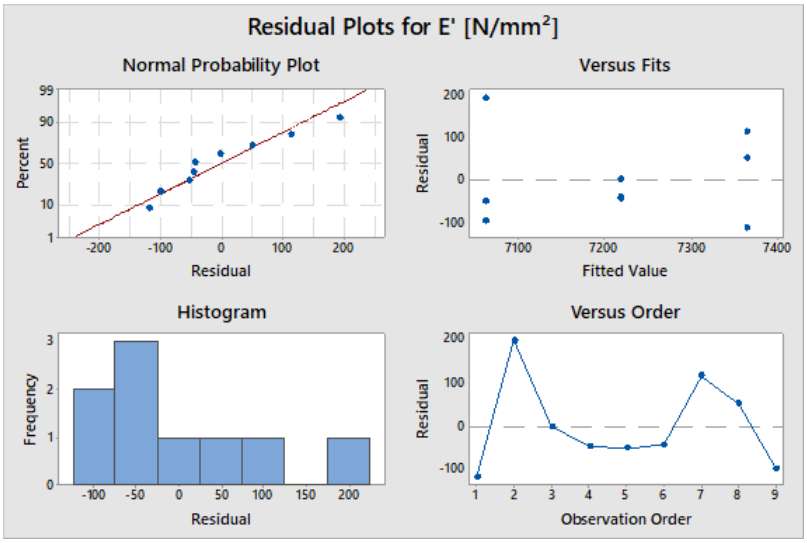
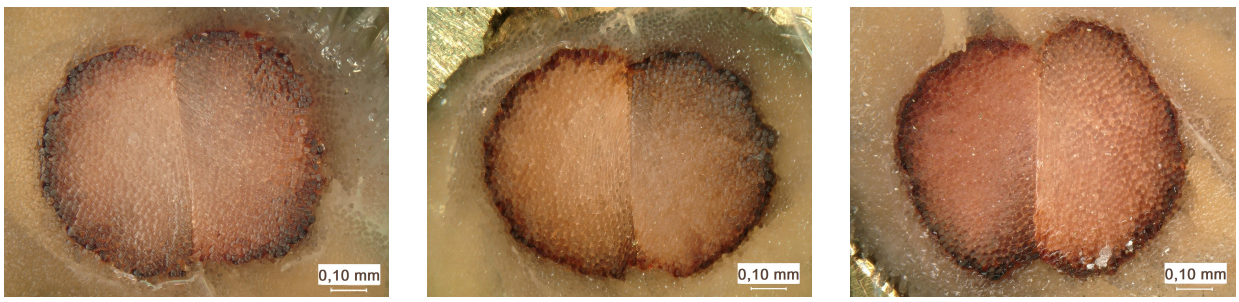


Figure 37: Analysis of residuals for E' over DPU %.

histogram. For all variables, the p-values are to be interpreted with care, as their accuracy is affected by the lack of normality. Besides that and given the small magnitude of the effect DPU % has on these variables, the power of this test is considerably low, which might prevent the detection of a significantly occurring effect for E'' and $\tan\delta$.

An additional investigation was carried out by obtaining microscopical images of the cords' cross-sections, in order to visually examine the penetration of the dip. Representative images of each level are shown in Figure 38.



(a) DPU = 3.43 % **(b)** DPU = 4.95 % **(c)** DPU = 6.57 %

Figure 38: Microscopic analysis of a cross section of the PET cords.

The dip seems to penetrate 2 to 3 layers of filaments in the outer region of the cord, with no visible distinction between cords with different DPU %.

All in consideration, the available results indicate that the change of the hysteretic properties with DPU % is not practically significant, allowing an increase in the tolerance level during the cord processing for this particular factor.

5 Conclusion

This project provided an insight on the hysteresis of tyre textile reinforcements.
A test procedure using the DMA technique was developed and optimised in order to investigate the hysteretic properties of textile cords.
These properties were analysed as functions of linear density and twist, using Nylon 6.6 cords, and of dip pick up percentage, using PET cords.
The procedure was also used to obtain a master curve, by evaluating the dynamic changes as a function of frequency and temperature.

For Nylon, twist showed a considerable effect on the storage and loss moduli, leading to decreasing values with increasing twist. However, both effects appeared to cancel out, resulting in comparable and very small values for the loss factor, indicating very little of the stored energy is dissipated as heat.
Linear density, however, indicated curvature for all three characteristic variables, positive for the storage and loss moduli, and negative for the loss factor. Regrettably, given that only three levels of linear density were analysed, proper modelling of the behaviour was not possible.

For PET, DPU % showed a very small impact on the hysteresis of the cords, only presenting a statistically significant effect in E', following a negative linear correlation. In addition, microscopical analysis of the cords' cross-sections showed no evidence of a difference in the dip penetration.

Additionally, following an extensive process of procedure optimisation, 10 isothermal curves in a small frequency range were obtained, derived from a single test, allowing the construction of a master curve and the respective shift factor function. For confidentiality reasons, the obtained master curve and shift factor function are not disclosed in this document.

Overall, this project allowed for a better understanding of textile cord behaviour under dynamic conditions as well as of some factors that influence it.

6 Assessment of the work done

6.1 Objectives achieved

The main goal of this project was to gain information on the viscoelastic and hysteresis behaviour of textile reinforcement cords. As such a test method was developed, applied and optimised for two materials, Nylon 6.6 and PET.
The effect of twist, linear density and DPU % was studied at 23 °C and 10 Hz, in order to provide some insight into the changes it imparts in the dynamical properties of cords. In addition, a single test procedure was developed and optimised, in a manner that would reduce testing time and allow the obtention of the characteristic dynamical variables as a function of temperature and frequency, in order to construct a master curve, needed for future projects.

6.2 Limitations and future work

The unprecedented character of this project was the main limitation, seeing as very little information was available in literature on the application of the DMA technique to cords. An additional limitation was obviously time, given not only the need for availability of the test system but also the extended testing time for some of the procedures.
As the MTS Acumen is being used in this type of dynamic characterization for the first time, it was also quite difficult and time-consuming to answer some unexpected technical issues and to deal with machine limitations, regarding resonance and measurement resolution.

Given the innovative aspect of this technique when applied for textile reinforcements, these studies were mainly preliminary, in order to obtain an overall impression of how the cord behaved and what factors had a significant effect on its hysteresis. As such several further studies are recommended, not only to obtain additional information but also as improvements to the current configuration:

- Expansion of the range of testing, for both the twist and linear density study and the DPU % study;
- Increase in number of replicates for at least the DPU % study, considering a reduced sample size has an impact not only on the normality assumption but especially on the capability of effect detection;

- Evaluation of the impact of the dipping process, given its possible effect on the cord's crystallinity;
- Application and optimisation of the test procedure for other reinforcement materials, such as rayon and hybrid;
- Characterization of the effect of the selected conditioning, pre-strain and amplitude in the hysteretic properties of the cords;
- Validation of the test procedure and further optimisation, with a possible standardization for other materials;
- Evaluation of the impact of the postprocessing of the results, comparing the use of the DIN method with the application of the sine regression and Fourier transform;
- Consideration of a force-controlled test mode, as opposed to the currently used strain-control, which ideally allows better correction parameters;
- Given tyre service conditions, expand these studies over a reasonable range of temperature and frequency, as they can interact with several other factors, altering their effect on cord behaviour.

6.3 Final assessment

This internship proved to be a great experience, not only professionally but also at a personal level. It was incredibly challenging, but in equal measure rewarding. It didn't just put to test my previously acquired knowledge, it invited me to find and assimilate as much information and skills as I could, allowing me to realize how much potential is in R&D. Despite all challenges, the obtained results proved valuable for Continental and will hopefully promote further investigations into this technique and the importance of the textile reinforcements in the tyre's damping capability.

References

[1] Continental Reifen Deutschland GmbH, "*Continental Corporation - Facts & Figures*," [Online] Available at https://www.continental-tires.com/car/company/about-us/corporate (Accessed February 2018).

[2] Continental Reifen Deutschland GmbH, "*Employee key figures and structure*," [Online] Available at https://www.continental-corporation.com/en/sustainability/employees/employee-key-figures-and-structure-63366 (Accessed February 2018).

[3] Continental Reifen Deutschland GmbH, "*Continental at a Glance - Key Facts*," [Online] Available at https://www.continental-corporation.com/en/career/working-at-continental/your-employer/continental-at-a-glance (Accessed February 2018).

[4] Continental Reifen Deutschland GmbH, "*Tyre Basics - Passenger Car Tyres*," 2013, available at https://blobs.continental-tires.com/www8/servlet/blob/85818/d2e4d4663a7c79ca81011ab47715e911/download-tire-basics-data.pdf?dl=t (Accessed February 2018).

[5] Continental Reifen Deutschland GmbH, "*Tyre Components - Image of the month August*," 2017, available at https://blobs.continental-tires.com/www8/servlet/blob/2041560/c0b1de2304d9a76dcf0f24657c93d043/img-8-bild-des-monats-data.png?dl=t (Accessed February 2018).

[6] B. E. Lindenmuth, "*An Overview of Tire Technology*," in *The Pneumatic Tire*, 2006, ch. 1.

[7] E. T. McDonel, "*Tire Cord and Cord-to-Rubber Bonding*," in *The Pneumatic Tire*, 2006, ch. 3.

[8] A. Aytaç, B. Yilmaz, and V. Deniz, "*Nylon 66/Polyester Hybrid Cords: 1. Design and Investigation of Properties*," vol. 12, no. 2, pp. 252–257, October 2011.

[9] X. Meng, M. Assaad, and M. Kavaturu, "*Impact of Pre-Strain, Initial Thermal Strain, and Viscoelasticity of Hybrid/Merged Cords on Tire Performance*," *Tire Science and Technology*, vol. 45, no. 4, p. 244–258, October-December 2017.

[10] D. B. Wootton, *The Application of Textiles in Rubber*, 2001.

[11] T. Kramer, "*Basics of Reinforcements*," in *Tire Academy - Technical Training*, 2018.

[12] A. Louis, J. W. M. Noordermeer, W. K. Dierkes, and A. Blume, "*Technologies for Polymer Cord / Rubber Adhesion in Tire Applications*," *Proceedings of 186th Technical Meeting ACS Rubber Division*, 2014.

[13] ASTM D885 / D885M - 03, *Standard Test Methods for Tire Cords, Tire Cord Fabrics, and Industrial Filament Yarns Made from Manufactured Organic-Base Fibers*. ASTM International, 2003.

[14] H. S. Aldhufairi and O. A. Olatunbosun, "*Developments in tyre design for lower rolling resistance: a state of the art review*," *Proceedings of the Institution of Mechanical Engineers, Part D: Journal of Automobile Engineering*, 2017.

[15] F. Tabaddor, S. K. Clark, R. N. Dodge, and J. M. Perraut, "*Viscoelastic Loss Characteristics of Cord-Rubber Composites*," *Tire Science and Technology*, vol. 14, no. 2, pp. 75–101, April-June 1986.

[16] P. R. Willett, "*Viscoelastic properties of tire cords*," *Journal of Applied Polymer Science*, vol. 19, no. 7, pp. 2005–2014, 1975.

[17] A. Demšar, V. Bukošek, and A. Kljun, "*Dynamic Mechanical Analysis of Nylon 66 Cord Yarns*," *Fibres & Textiles in Eastern Europe*, vol. 18, no. 4, pp. 29–33, 2010.

[18] B. K. Samui, M. P. Prakasan, D. Chakrabarty, and R. Mukhopadhyay, "*Hysteresis characteristics of high modulus low shrinkage polyester tire yarn and cord*," *Rubber Chemistry and Technology*, vol. 84, no. 4, pp. 565–579, 2011.

[19] Perkin Elmer, "*Dynamic Mechanical Analysis (DMA) - A Beginner's Guide*."

[20] G. Frunză and E. N. Diaconescu, "*Hysteresis and mechanical fatigue*," *The Annals of University Dunărea de Jos of Galati*, vol. 8, no. 12, pp. 61–66, 2006.

[21] W. D. Callister, *Materials Science and Engineering: An Introduction*, 7th ed. John Wiley & Sons, Inc., 2007.

[22] M. A. Meyers and K. K. Chawla, *Mechanical Behavior of Materials*, 2nd ed. Cambridge University Press, 2009.

[23] MTS Systems Corporation, "*Test Method TechNote - Rubber*," 2018.

[24] DIN 53513:1990-03, *Prüfung von Kautschuk und Elastomeren; Bestimmung der viskoelastischen Eigenschaften von Elastomeren bei erzwungenen Schwingungen außerhalb der Resonanz*. Deutsches Institut für Normung, 1990.

[25] MTS Systems Corporation, "*High-Force Dynamic Mechanical Analysis (DMA)*."

[26] Société de Technologie Michelin, "*The Tyre - Rolling resistance and fuel savings*," 2003.

[27] TestResources, "*G9 Tensile Wire Capstan Grip 560 lbf*," [Online] Available at https://www.testresources.net/images/accessories/tensile-grips/g9-capstan-grip.jpg (Accessed May 2018).

[28] STAHLWILLE Eduard Wille GmbH & Co. KG, "*Product Catalogue*," 2018.

[29] Thwing-Albert Instrument Company, "*TA149 Pneumatic Grip*."

[30] Mettler-Toledo AG, "*Thermal Analysis of Polymers*."

[31] Y. D. Kwona, R. K. Sharma, and D. C. Prevorsek, "*Viscoelastic Properties of Tire Cords Under Conditions of Rolling Tires*," in *Tire Reinforcement and Tire Performance, ASTM STP 694*. American Society for Testing and Materials: Oxford University Press, 1979, pp. 239–262.

[32] A. Ayta, B. Yilmaz, and V. Deniz, "*Effects of Linear Density and Twist Level on the Mechanical Properties of Nylon 6.6 Tyre Cords*," *Fibers and Polymers*, vol. 11, no. 2, pp. 309–315, April 2010.

[33] K. P. Menard and N. R. Menard, "*Dynamic Mechanical Analysis in the Analysis of Polymers and Rubbers*," *Encyclopedia of Polymer Science and Technology*, pp. 1–33, 2015.

[34] Perkin Elmer, "*Dynamic Mechanical Analysis Basics: Part 2 Thermoplastic Transitions and Properties* ."

Appendix A Linear density and twist study

Design of experiments

The design of experiments for this study is shown in Table 5, as well as the obtained estimated limit values. An initial design included the missing combination of a high twist with 470 dtex, which justifies the skipped Run Order values.

Table 5: Design of experiments for the linear density and twist study, as well as the corresponding limit value estimates.

Run Order	Block	LD [dtex]	Twist Level	Twist [tpm]	Twist Factor	E′ [N/mm²]	E″ [N/mm²]	tan δ
1	3	1400	high	378	200	3563.7	295.3	0.0830
2	3	470	low	250	77	4631.6	363.1	0.0785
3	3	940	low	231	100	4071.4	350.1	0.0862
4	3	940	standard	350	152	3300.6	289.6	0.0878
5	3	940	high	461	200	3006.1	269.9	0.0899
6	3	470	standard	420	129	4204.6	315.9	0.0751
8	3	1400	standard	290	153	3943.8	305.6	0.0776
9	3	1400	low	170	90	4875.4	378.3	0.0776
10	2	470	low	250	77	4538.0	360.5	0.0795
12	2	1400	high	378	200	3213.1	282.3	0.0879
13	2	470	standard	420	129	4197.6	316.4	0.0754
14	2	1400	low	170	90	4815.2	370.3	0.0769
15	2	1400	standard	290	153	3825.0	308.8	0.0808
16	2	940	standard	350	152	3347.0	289.5	0.0865
17	2	940	high	461	200	2889.4	261.9	0.0907
18	2	940	low	231	100	3846.5	340.6	0.0886
19	4	1400	high	378	200	3320.6	292.5	0.0882
20	4	1400	low	170	90	4776.2	374.6	0.0785
21	4	940	high	461	200	2875.4	261.4	0.0910
22	4	940	standard	350	152	3419.3	294.1	0.0860
23	4	1400	standard	290	153	3976.3	303.8	0.0764
24	4	940	low	231	100	3849.5	336.5	0.0875
25	4	470	low	250	77	4593.1	364.1	0.0793

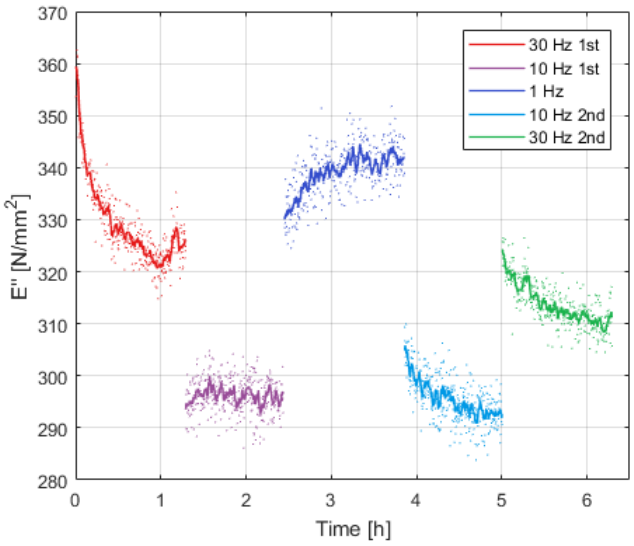
Table 5: Design of experiments for the linear density and twist study, as well as the corresponding limit value estimates.

Run Order	Block	LD [dtex]	Twist Level	Twist [tpm]	Twist Factor	E′ [N/mm²]	E″ [N/mm²]	tan δ
26	4	470	standard	420	129	3925.6	311.9	0.0795
28	5	1400	standard	290	153	3980.6	314.0	0.0789
29	5	470	standard	420	129	3938.1	304.4	0.0774
30	5	1400	high	378	200	3295.0	294.7	0.0895
31	5	470	low	250	77	4462.8	362.1	0.0809
32	5	940	high	461	200	2821.6	263.9	0.0936
34	5	940	low	231	100	3507.8	333.6	0.0952
35	5	940	standard	350	152	3421.9	294.0	0.0859
36	5	1400	low	170	90	4585.5	367.3	0.0802
38	1	940	low	231	100	3847.8	345.5	0.0900
39	1	1400	standard	290	153	3901.2	310.2	0.0795
40	1	470	standard	420	129	3602.7	311.7	0.0865
41	1	940	high	461	200	2553.7	250.8	0.0983
42	1	1400	low	170	90	4999.6	388.3	0.0777
43	1	940	standard	350	152	3282.8	290.9	0.0886
44	1	470	low	250	77	4361.2	355.6	0.0817
45	1	1400	high	378	200	3216.4	292.2	0.0909

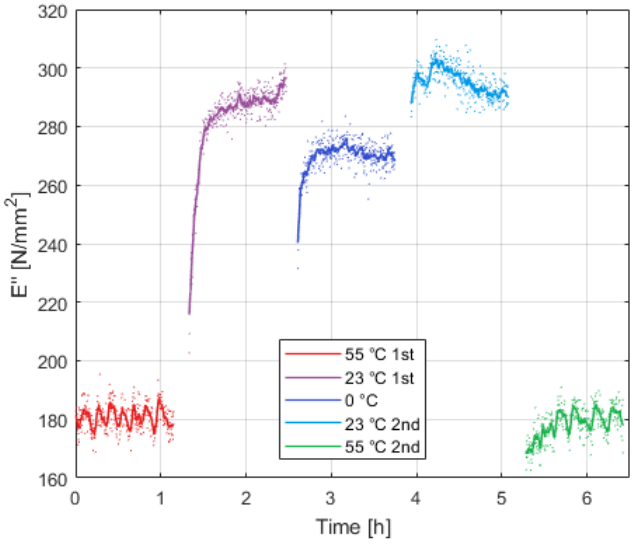
Appendix B Master curve construction

Throughout the main body of the thesis, E' is shown as a representative of the results. For those situations, the results obtained for E'' and $\tan\delta$ are shown in this appendix.

Initial frequency and temperature studies



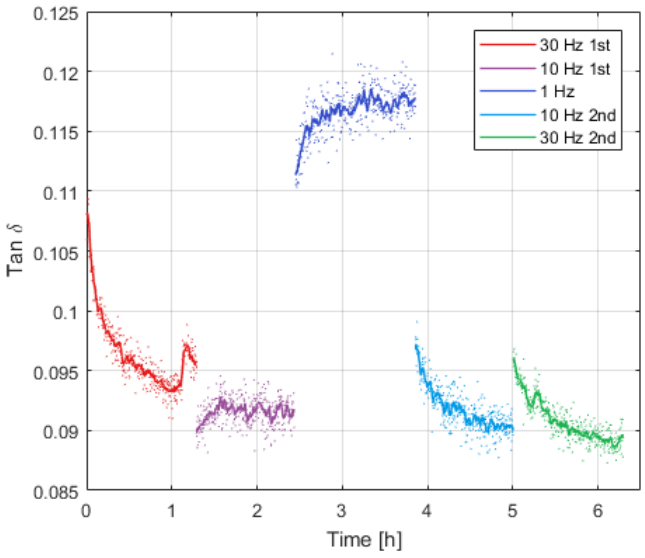
(a)



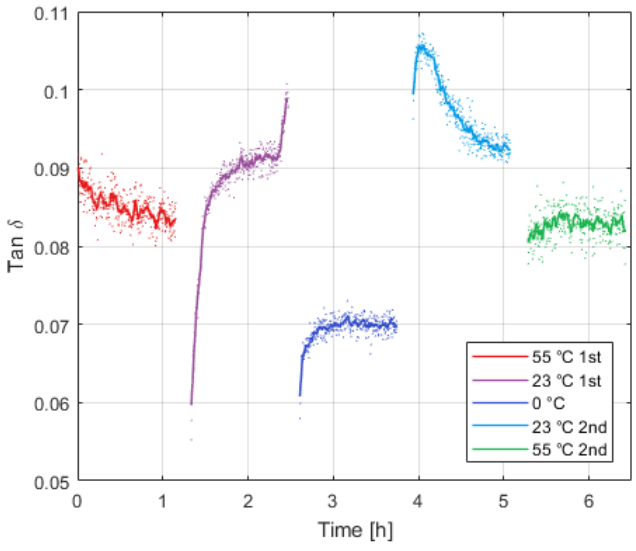
(b)

Figure 39: Representation of E'' for the frequency (a) and temperature (b) steps test procedure.

From Figures 41 and 42, one can conclude, as before, that the transient behaviour is reversible and the steady state is independent of the testing history. In addition, an easier handling is observed for frequency sweeps, with the initial more extreme setting working as a conditioning block, especially for decreasing frequencies.



(a)



(b)

Figure 40: Representation of $\tan\delta$ for the frequency (a) and temperature (b) steps test procedure.

Comparative frequency and temperature sweep

The results obtained for E'' and $\tan\delta$ concerning the four procedures are shown in Figures 41 and 42. These results are adjusted over the time frame of the increasing temperature sweep (blue line) in order to allow comparison between the tests.

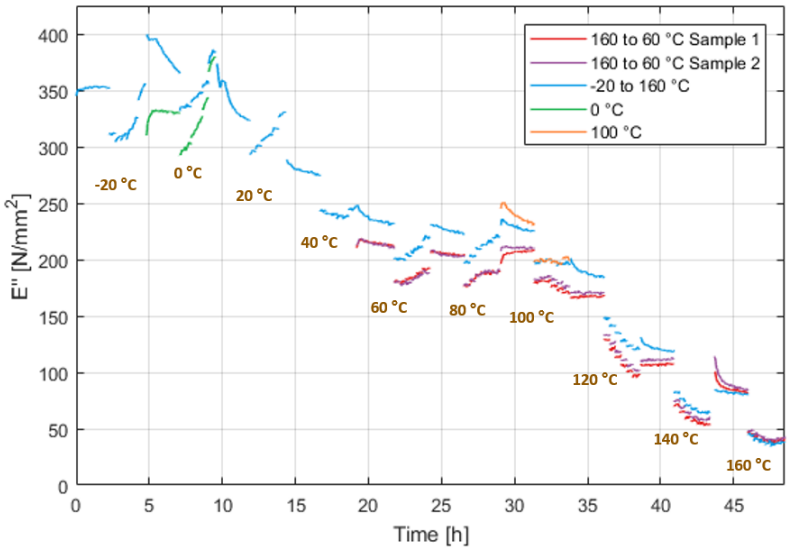


Figure 41: Comparative results for E'' from the nested frequency sweeps in a temperature sweep procedures.

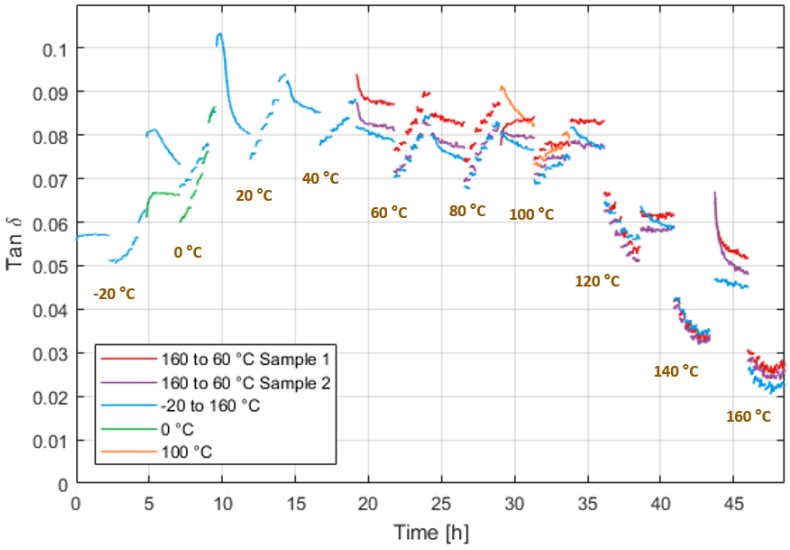


Figure 42: Comparative results for $\tan\delta$ from the nested frequency sweeps in a temperature sweep procedures.

Fitting results

The limit values obtained via asymptotic regression fitting are available in Table 6, and represented over temperature in Figures 31(a), 31(b) and 31(c).

Table 6: Obtained fitted values from the selected frequency and temperature sweep.

Frequency [Hz]	**T [°C]**	**E′ [N/mm²]**	**E″ [N/mm²]**	**tan δ**
30	-20	6175.2	352.8	0.057
	0	5289.5	333.6	0.064
	20	4021.4	321.9	0.080
	40	3230.7	275.0	0.085
	60	2932.9	231.6	0.075
	80	2992.1	217.8	0.074
	100	2933.5	221.3	0.076
	120	2397.3	179.2	0.075
	140	2013.4	118.4	0.058
	160	1785.3	75.9	0.028
17	-20	6082.0	311.5	0.051
	0	4885.2	335.2	0.069
	20	3906.3	296.3	0.076
	40	3091.4	243.3	0.079
	60	2836.4	200.6	0.071
	80	2912.0	197.5	0.068
	100	2849.8	196.6	0.069
	120	2308.1	147.6	0.064
	140	1947.1	82.2	0.042
	160	1723.7	44.6	0.026

Table 6: Obtained fitted values from the selected frequency and temperature sweep.

Frequency [Hz]	**T [°C]**	**E′ [N/mm²]**	**E″ [N/mm²]**	**tan δ**
9.7	-20	6011.6	309.6	0.052
	0	4813.2	336.2	0.070
	20	3799.6	301.2	0.079
	40	3021.2	240.5	0.080
	60	2781.8	200.4	0.072
	80	2857.6	202.9	0.071
	100	2809.2	198.8	0.071
	120	2272.7	141.3	0.062
	140	1926.7	76.1	0.039
	160	1709.5	40.9	0.024
5.5	-20	5899.2	313.9	0.053
	0	4741.6	345.8	0.073
	20	3732.2	306.9	0.082
	40	2953.9	239.9	0.081
	60	2741.5	200.4	0.074
	80	2816.3	209.4	0.074
	100	2763.3	200.1	0.072
	120	2240.4	135.0	0.060
	140	1905.2	70.9	0.037
	160	1695.1	38.7	0.023
3.1	-20	5853.5	316.4	0.054
	0	4661.9	347.9	0.075
	20	3654.3	310.4	0.085
	40	2892.1	238.9	0.083
	60	2691.7	207.8	0.077
	80	2763.3	213.2	0.077
	100	2713.2	198.1	0.073
	120	2204.4	128.1	0.058
	140	1884.5	67.7	0.036
	160	1682.3	39.8	0.024

Table 6: Obtained fitted values from the selected frequency and temperature sweep.

Frequency [Hz]	**T [°C]**	**E′ [N/mm²]**	**E″ [N/mm²]**	**tan δ**
1.8	-20	5762.2	328.7	0.057
	0	4592.6	359.3	0.078
	20	3589.4	316.2	0.088
	40	2845.6	239.4	0.084
	60	2650.8	211.0	0.080
	80	2720.9	216.0	0.079
	100	2671.9	196.1	0.073
	120	2177.0	123.5	0.057
	140	1869.6	64.7	0.035
	160	1672.8	36.4	0.022
1	-20	5668.4	363.8	0.064
	0	4498.6	385.1	0.086
	20	3520.3	332.8	0.094
	40	2793.8	244.9	0.088
	60	2612.6	219.7	0.084
	80	2673.3	220.0	0.082
	100	2625.2	196.8	0.075
	120	2144.0	120.7	0.056
	140	1849.5	64.5	0.035
	160	1660.4	37.6	0.023

Appendix C DPU % study

Design of experiments

The design of experiments for this study is shown in Table 7, as well as the obtained estimated limit values.

Table 7: Design of experiments for the DPU % study, as well as the corresponding limit value estimates.

Run Order	DPU [%]	E' [N/mm^2]	E'' [N/mm^2]	$\tan\delta$
1	3.43	7246.8	314.9	0.0435
2	6.57	7257.5	298.7	0.0412
3	4.95	7217.0	290.4	0.0403
4	4.95	7171.9	296.7	0.0414
5	6.57	7010.7	311.9	0.0446
6	3.43	7478.6	304.6	0.0408
7	4.95	7174.9	309.7	0.0432
8	3.43	7415.0	313.2	0.0423
9	6.57	6963.1	307.6	0.0443

One-way ANOVA

For the analysis of variance, the following considerations were made:

Method

Null hypothesis	All means are equal
Alternative hypothesis	At least one mean is different
Significance level	$\alpha = 0.05$

Equal variances were assumed for the analysis.

Factor Information

Factor	Levels	Values
DPU [%]	3	3.43, 4.95, 6.57

The MINITAB output obtained from the one-way ANOVA performed with DPU % as a factor and E' as the response is grouped in Table 8.

Table 8: ANOVA output for E' as function of DPU %.

Analysis of Variance

Source	DF	Adj SS	Adj MS	F-value	P-value
DPU [%]	2	141052	70526	5.29	0.047
Error	6	79921	13320		
Total	8	220974			

Model Summary

S	R-sq	R-sq (adj)	R-sq (pred)
115.413	63.83 %	51.78 %	18.62 %

Means

DPU [%]	N	Mean	StDev	95 % CI
3.43	3	7380.1	119.8	(7217.1, 7543.2)
4.95	3	7188.0	25.2	(7024.9, 7351.0)
6.57	3	7077.1	158.0	(6914.0, 7240.1)
Pooled StDev = 115.413				

The MINITAB output obtained from the one-way ANOVA performed with DPU % as a factor and E'' as the response is grouped in Table 9.

Table 9: ANOVA output for E'' as function of DPU %.

Analysis of Variance

Source	DF	Adj SS	Adj MS	F-value	P-value
DPU [%]	2	216.6	108.30	1.87	0.233
Error	6	346.7	57.78		
Total	8	563.3			

Model Summary

S	R-sq	R-sq (adj)	R-sq (pred)
7.60163	38.45 %	17.93 %	0.00 %

Means

DPU [%]	N	Mean	StDev	95 % CI
3.43	3	310.88	5.49	(300.14, 321.62)
4.95	3	298.94	9.87	(288.20, 309.68)
6.57	3	306.08	6.77	(295.34, 316.82)
Pooled StDev = 7.60163				

The MINITAB output obtained from the one-way ANOVA performed with DPU % as a factor and $\tan\delta$ as the response is grouped in Table 10.

Table 10: ANOVA output for $\tan\delta$ as function of DPU %.

Analysis of Variance

Source	DF	Adj SS	Adj MS	F-value	P-value
DPU [%]	2	0.000004	0.000002	0.90	0.456
Error	6	0.000015	0.000002		
Total	8	0.000019			

Model Summary

S	R-sq	R-sq (adj)	R-sq (pred)
0.0015719	23.02 %	0.00 %	0.00 %

Means

DPU [%]	N	Mean	StDev	95 % CI
3.43	3	0.042205	0.001366	(0.039985, 0.044426)
4.95	3	0.041657	0.001468	(0.039437, 0.043878)
6.57	3	0.04334	0.00184	(0.04112, 0.04556)
Pooled StDev = 0.00157189				

Tukey pairwise comparisons

In order to determine which means showed significant differences between each other, a post hoc Tukey comparison test was carried out for E'.

Grouping Information Using the Tukey Method and 95 % Confidence

DPU [%]	N	Mean	Grouping
3.43	3	7380.1	A
4.95	3	7188.0	A B
6.57	3	7077.1	B

Means that do not share a letter are significantly different.

Simple linear regression

Lastly, the behaviour of the storage modulus was fitted with a linear regression, for which the following considerations were made:

Method

Continuous predictor standardization
Subtract the mean

Predictor	Mean
DPU [%]	4.98333

The MINITAB output obtained from the Regression Analysis performed with DPU % as a factor and E' as the response is grouped in Table 11.

Table 11: Regression output for E' as function of DPU %.

Analysis of Variance

Source	DF	Adj SS	Adj MS	F-Value	P-Value
Regression	1	136917	136917	11.40	0.012
DPU [%]	1	136917	136917	11.40	0.012
Error	7	84057	12008		
Lack-of-Fit	1	4136	4136	0.31	0.598
Pure Error	6	79921	13320		
Total	8	220974			

Model Summary

S	R-sq	R-sq (adj)	R-sq (pred)
109.582	61.96 %	56.53 %	28.08 %

Coded Coefficients

Term	Coef	SE Coef	T-Value	P-Value	VIF
Constant	7215.1	36.5	197.53	0.000	
DPU [%]	-96.2	28.5	-3.38	0.012	1.00

Regression Equation in Uncoded Units

$$E' \text{ [N/mm}^2\text{]} = 7694 - 96.2 \text{ DPU [\%]}$$

Fits and Diagnostics for Unusual Observations

Obs	E' [N/mm^2]	Fit	Resid	Std Resid		
2	7257.5	7062.4	195.1	2.10	R	Large residual